R 740

Technical Report

INFLUENCE OF END-CLOSURE STIFFNESS ON BEHAVIOR OF CONCRETE CYLINDRICAL HULLS SUBJECTED TO HYDROSTATIC LOADING

October 1971

Sponsored by

NAVAL FACILITIES ENGINEERING COMMAND

NAVAL CIVIL ENGINEERING LABORATORY

Port Hueneme, California 93043

57

INFLUENCE OF END-CLOSURE STIFFNESS ON BEHAVIOR OF CONCRETE CYLINDRICAL HULLS SUBJECTED TO HYDROSTATIC LOADING

Technical Report R-740

3.1610-1

by

L. F. Kahn

ABSTRACT

Twelve model concrete cylindrical hulls were subjected to hydrostatic loading to determine the influence of end-closure stiffness on implosion pressure and strain behavior of the cylinders. Results showed that variation of end-closure stiffness did not reduce the implosion pressure below that of a cylinder with a free end condition or below the implosion pressure predicted by elastic thick-wall theory. To vary the closure stiffness, concrete hemisphere and steel plate end closures were used to simulate free, pinned, beveled, and fixed end conditions. Strain variations along the length of the cylinders indicated that the influence of the closure was limited to a distance of one diameter from the closure. Recommendations are presented to aid in the design of concrete cylindrical hulls.

Approved for public release, distribution unlimited.

Copies available at the National Technical Information Service (NTIS), Sills Building, 5285 Port Royal Road, Springfield, Va. 22151

Unclassified

Security Classification

DOCUMENT CONTROL DATA - R & D

Security classification of title, body of abstract and indexing annotation must be entered when the overall report is classified)

1 ORIGINATING ACTIVITY *(Corporate author)* Naval Civil Engineering Laboratory Port Hueneme, California 93043	2a. REPORT SECURITY CLASSIFICATION Unclassified 2b. GROUP

3 REPORT TITLE

INFLUENCE OF END-CLOSURE STIFFNESS ON BEHAVIOR OF CONCRETE CYLINDRICAL HULLS SUBJECTED TO HYDROSTATIC LOADING

4 DESCRIPTIVE NOTES *(Type of report and inclusive dates)*

Not final; July 1969–April 1971

5 AUTHOR(S) *(First name, middle initial, last name)*

L. F. Kahn

6 REPORT DATE October 1971	7a. TOTAL NO OF PAGES 53	7b. NO OF REFS 4
8a CONTRACT OR GRANT NO b. PROJECT NO 3.1610-1 c. d.	9a. ORIGINATOR'S REPORT NUMBER(S) TR-740 9b. OTHER REPORT NO(S) *(Any other numbers that may be assigned this report)*	

10 DISTRIBUTION STATEMENT

Approved for public release; distribution unlimited.

11 SUPPLEMENTARY NOTES	12. SPONSORING MILITARY ACTIVITY Naval Facilities Engineering Command Washington, D. C. 20390

13 ABSTRACT

Twelve model concrete cylindrical hulls were subjected to hydrostatic loading to determine the influence of end-closure stiffness on implosion pressure and strain behavior of the cylinders. Results showed that variation of end-closure stiffness did not reduce the implosion pressure below that of a cylinder with a free end condition or below the implosion pressure predicted by elastic thick-wall theory. To vary the closure stiffness, concrete hemisphere and steel plate end closures were used to simulate free, pinned, beveled, and fixed end conditions. Strain variations along the length of the cylinders indicated that the influence of the closure was limited to a distance of one diameter from the closure. Recommendations are presented to aid in the design of concrete cylindrical hulls.

DD FORM 1 NOV 65 1473 (PAGE 1)

S/N 0101-807-6801

Unclassified

Security Classification

Unclassified

Security Classification

14 KEY WORDS	LINK A		LINK B		LINK C	
	ROLE	WT	ROLE	WT	ROLE	WT
Underwater construction						
Concrete cylindrical hulls						
Hydrostatic tests						
Implosion pressure						
End closures						
Model concrete cylinders						
Cylindrical hulls						
End-closure stiffness						
Pressure-resistant structures						
Concrete shells						
Thick-wall shells						

DD FORM 1 NOV 65 1473 (BACK)

(PAGE 2)

Unclassified

Security Classification

CONTENTS

BLANK PAGE

INTRODUCTION

The prospective use of concrete cylindrical hulls for undersea installations requires that some form of end closure be provided. The closure may be a shell or plate made of concrete or another material; or the closure may be another structure to which the cylindrical hull connects, such as a sphere. The difference in stiffness between the cylinder and the closure will affect the structural behavior of the cylindrical hull.

The primary objective of this investigation was to determine the effect of the end-closure stiffness on the structural behavior of thick-walled concrete cylindrical hulls subjected to hydrostatic loading. The effect of the end closure was studied by testing experimental models and by analyzing the models with a finite element technique. The secondary objective was to compare the experimental behavior with the analytical behavior to determine the accuracy of the analytical method.

The ultimate purpose of this research is to aid in developing design guidelines for the accurate and safe design of undersea concrete structures. Applications for such undersea structures include stations to monitor ocean activities, nuclear reactor containment structures, transportation tunnels, mineral refinement plants, and oil drilling enclosures.

BACKGROUND

Previous experimental research at the Naval Civil Engineering Laboratory (NCEL) on model cylindrical hulls determined the effect of the cylinder length-to-outside-diameter ratio (L/D_o)* on the strain behavior and implosion pressure of the hulls and indicated the minimum length-to-diameter ratio which approximates a cylinder of "infinite"** length.[1] Fourteen concrete cylindrical hulls were tested. These hulls had an outside diameter of 16 inches and a 2-inch wall thickness. End closures

* A foldout list of symbols is included after References.

** An "infinitely long" cylinder is one in which radial displacements are uniform along the length.

were concrete hemispheres with a 16-inch outside diameter and 2-inch wall thickness. The L/D_o ratio was varied from 0.5 to 8.0. Principal findings of the study were that:

1. A cylinder with an L/D_o ratio of 2.0 or greater can be considered infinitely long.
2. Exterior hoop strains were nearly uniform beyond a distance equal to or greater than one outside diameter from the cylinder end.
3. Cylinders with an L/D_o ratio greater than 2.0 imploded at a pressure loading of approximately 2,500 psi, which was conservatively predicted with Lamé's elastic thick-wall theory.
4. Hoop strains around the circumference of a cylinder at midlength were not uniform; apparently a flat spot developed which eventually resulted in the hull failure.

Along with the experimental investigation, the cylinders were analyzed with a finite element method developed by E. L. Wilson.[2] The finite element analysis indicated behavior similar to that determined in the experimental findings.

EXPERIMENTAL PROGRAM

Scope

This investigation was principally an experimental study of 12 model concrete cylindrical hulls with concrete hemisphere and steel plate end closures. The closures were used to create various amounts of fixity at the cylinder ends. The only intended variable in the experiment was the closure stiffness. The structural behavior of the cylinders was studied by measuring the exterior strain of the models as they were subjected to hydrostatic pressure loading. All cylinders were tested to implosion.

The experiments were designed to yield sufficient data to show the influence of end-closure stiffness on the structural behavior. These data were then compared with the results from a finite element analysis of the cylinder models to determine the difference between actual and theoretical behavior. The analytical and experimental findings were used to formulate the recommendations for design guidelines.

Design of Specimens

The 12 model concrete cylinders were similar to those fabricated in the previous research study,[1] with a length-to-diameter ratio (L/D_o) of 2.0 and thickness-to-diameter ratio (t/D_o) of 0.125. The cylinders had an outside diameter of 16 inches, wall thickness of 2 inches, and length of 32 inches.

Four end-fixity conditions were used and ranged from approximately no end restraint to infinite restraint (Table 1). Two cylinders each were tested with free end and pinned end conditions, and four cylinders each were tested with beveled end and fixed end conditions.

To produce the least restraint, concrete hemispheres with a 16-inch outside diameter and 1-inch wall thickness were bonded with epoxy to each end of a cylinder (specimens 1 and 2). Elastic thick-wall theory predicted that the 1-inch-thick hemisphere would have a radial deflection 0.95 times the deflection of the 2-inch-thick cylinder; therefore, the hemispherical end closure was approximately 5% stiffer than the cylinder. Because of this small difference, the hemispherical closure would produce little end restraint, and the cylindrical hull would respond to hydrostatic loading in a manner similar to that of a portion of an infinitely long hull. Hence, hemispherical end closures having a wall thickness one-half that of the cylinder were considered as providing free end restraint conditions.

Specimens 3 through 8 had one end of the cylinder capped with a 16-inch-OD, 1-inch-thick concrete hemisphere and the other end with a steel plate closure. Specimens 9 through 12 had one end capped with a 16-inch-OD x 2-inch-thick concrete hemisphere and the other end with a steel plate closure. The 1-inch-thick hemisphere was used at one end so that any variation in the structural behavior along the length of the cylinder would be caused by the various plate closures and the cylinder would respond as a semi-infinitely long cylinder with one end restrained. Even though the 1-inch hemisphere would provide the desired free restraint conditions, it would produce an edge bearing effect which might influence the hull implosion behavior. The 2-inch hemispheres were used to avoid edge bearing effects, although the thicker hemispheres would somewhat restrain cylinder deflection.

A cylinder length-to-diameter ratio of 2.0 was chosen because, as determined by Haynes and Ross,[1] a cylinder with an L/D_o ratio of 2.0 or greater behaved as an infinitely long cylinder. Therefore, any variation in structural behavior caused by varying the end closures could be assumed to be the result of changing the restraint at one end of the cylinder and not of any influence at the other.

Table 1. End-Closure Restraint Conditions

Specimen Nos.	Closure Systems	Radial Deflection	End Rotation	Diagram
1, 2	free end	unrestrained	unrestrained	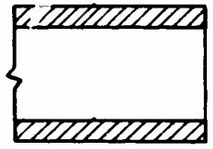
3, 4	pinned end	restrained	unrestrained	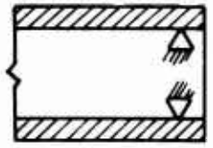
5, 6, 9, 10	beveled end	partially restrained	partially restrained	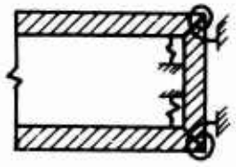
7, 8, 11, 12	fixed end	restrained	restrained	

The steel plate end closures are shown in Figure 1. Specimens 3 and 4 had a steel plate end closure which simulated a pinned end condition. The closure was designed to permit nearly free rotation while preventing radial displacement. As shown in Figure 2, a steel ring was grouted between the bearing edge of the closure and the concrete cylinder. This ring prevented excessively high bearing stresses. Because the ring was grooved and flexible, it did not restrain the cylinder rotation.

Specimens 5, 6, 9, and 10 had a beveled steel plate end closure (Figure 3). Both the plate and the cylinder were fabricated with a 45-degree beveled edge. This configuration was designed to partially restrain both the radial deflection and rotation of the cylinder. The beveled condition also represented a design which might be practical for movable closures.

The steel plate closure for specimens 7, 8, 11, and 12 was designed to ensure full fixity of the cylinder end by restraining radial deflection and rotation. The fixed end closure (Figure 4) fit around the cylinder end so that the cylinder penetrated the plate 3 inches.

Fabrication of Specimens

The concrete (technically a microconcrete or mortar, because the largest aggregate passed a no. 4 sieve) used to cast both the cylinders and hemispheres had a compressive strength ranging from 5,910 to 10,640 psi and elastic moduli from 2.4×10^6 to 3.8×10^6 psi. Details of the mix design and physical properties of the concrete are presented in Appendix A.

The cylinders were cast vertically in rigid steel molds (Figure 5). The molds were machined to diameter tolerances of ±1/32 inch, and could be separated into parts for easy removal from the cast cylinder.

The two cylinder sections which were to have the same type end closure were cast on the same day but from different batches of concrete. During casting, the concrete was vibrated both internally and externally to assure good compaction and homogeniety. The molds were removed one day after casting, and the sections were cured in a fog room at 100% RH and $73^{\circ}F$ until the concrete aged 28 days. Upon removal from the fog room, the cylinders were stored at room conditions within a building while being instrumented and having the end closures attached.

The concrete hemispheres were cast in rigid aluminum molds. External vibration was used during casting to ensure compaction. The hemispheres were cured under the same conditions as were the concrete cylinder sections. The flat edges on the cylinders and hemispheres were ground smooth and plane by rotating the sections on a sheet of plate glass covered with water and silicon carbide grit no. 60.

(a) Pinned.

(b) Beveled.

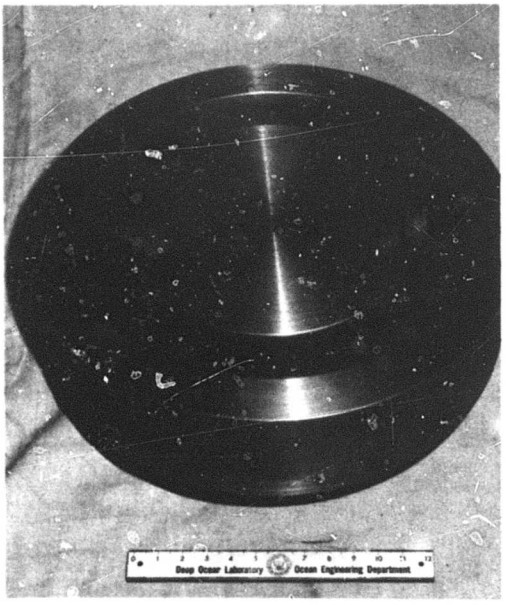

(c) Fixed.

Figure 1. Steel plate end closures.

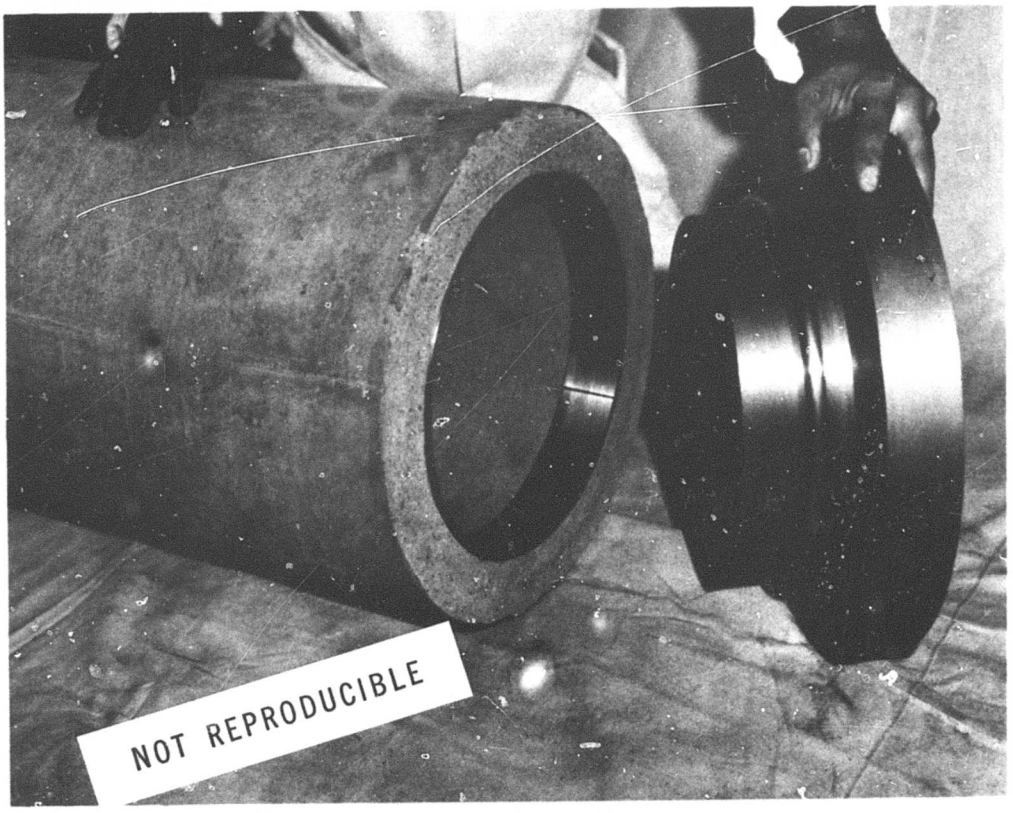

Figure 2. Pinned end closure with bearing ring in cylinder.

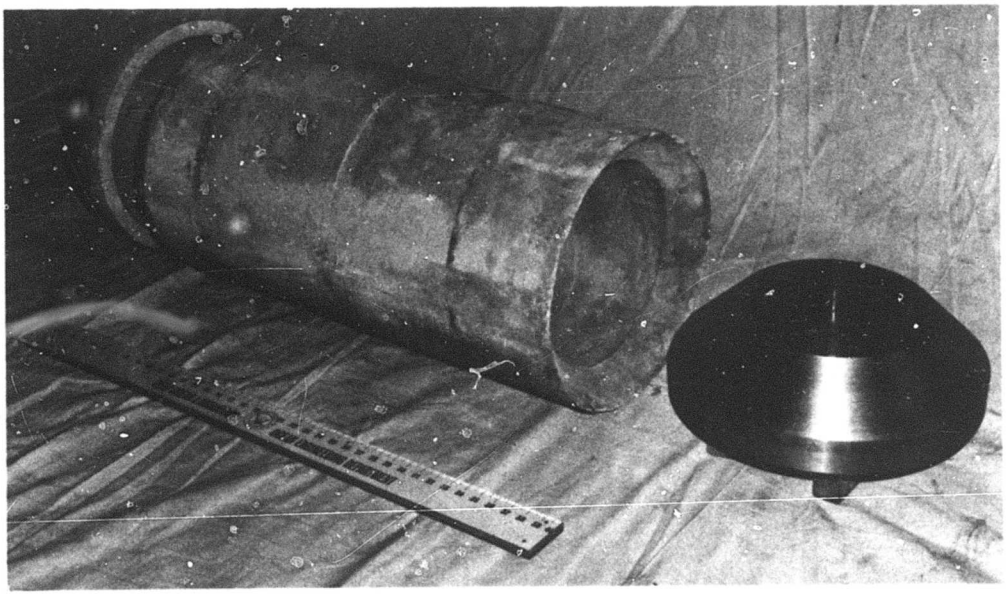

Figure 3. Beveled end closure with cylinder and hemispherical end.

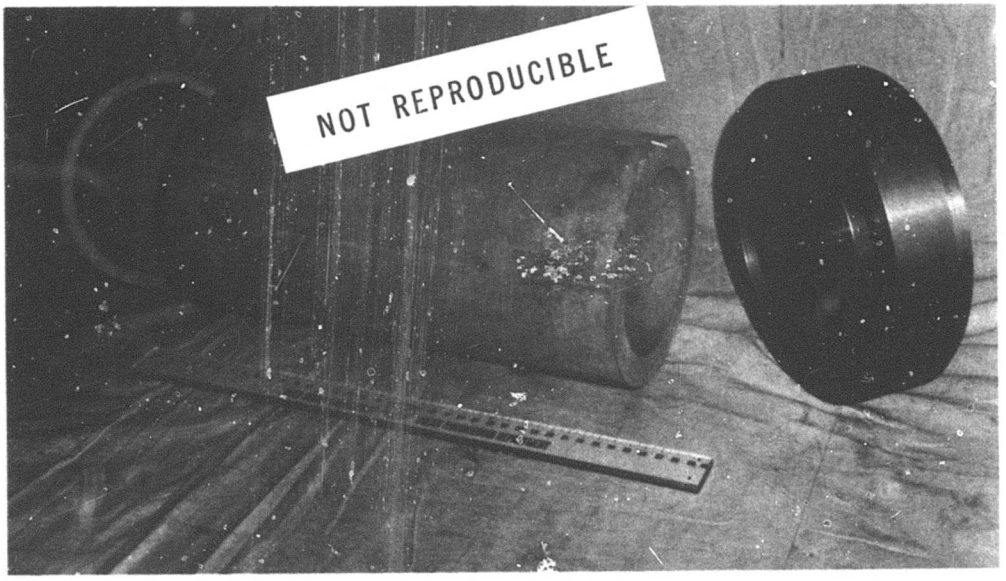

Figure 4. Fixed end closure with cylinder and hemispherical end.

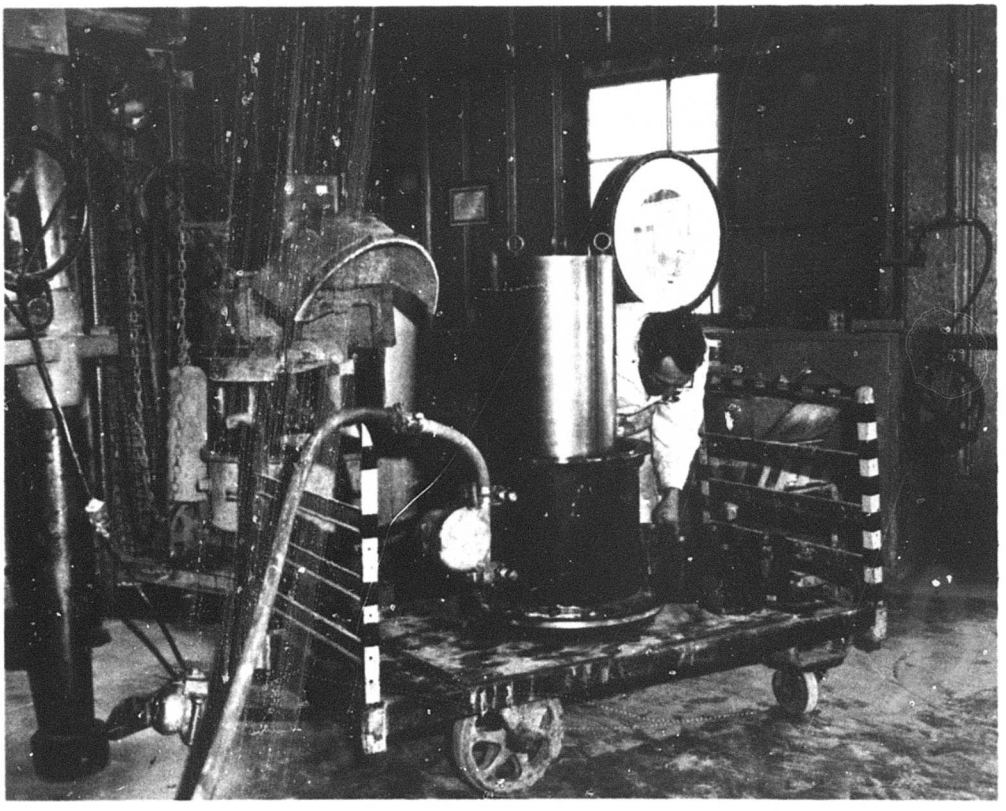

Figure 5. Rigid steel mold partially assembled for casting.

The steel end closures were machined from 6-inch-thick A36 steel plate. Dimensions were within a tolerance of ±0.005 inch. Drawings of the plate closures are shown in Appendix B.

The end closures were epoxy-bonded to the cylinders while the cylinder was in a vertical position. The hemispherical closures were placed first (Figure 6), using a high-strength epoxy (Furane Plastics, Epocast 8288). After 1 week the cylinder was inverted, and the other closure was fitted in place. For specimens 1 and 2, the second hemisphere was epoxy-bonded to the edge of the cylinder. For specimens 3 and 4, steel bearing rings were grouted to the cylinder interior surface with a neat cement paste, then the pinned end closure was epoxy-bonded to the edge of the cylinder. The pinned end closure fit snugly into the bearing ring. The beveled end closure was epoxy-bonded to specimens having beveled edges (Figure 7) with a bond approximately 0.020 inch thick. To attach the fixed end closure, the deep groove of the closure was painted with a thick coat of a low-viscosity, steel-filled epoxy (Furane Plastics, Epibond 154) and the closure was lowered onto the cylinder. The epoxy flowed sufficiently to ensure that the bond between the closure and the cylinder was complete and that the closure was correctly seated.

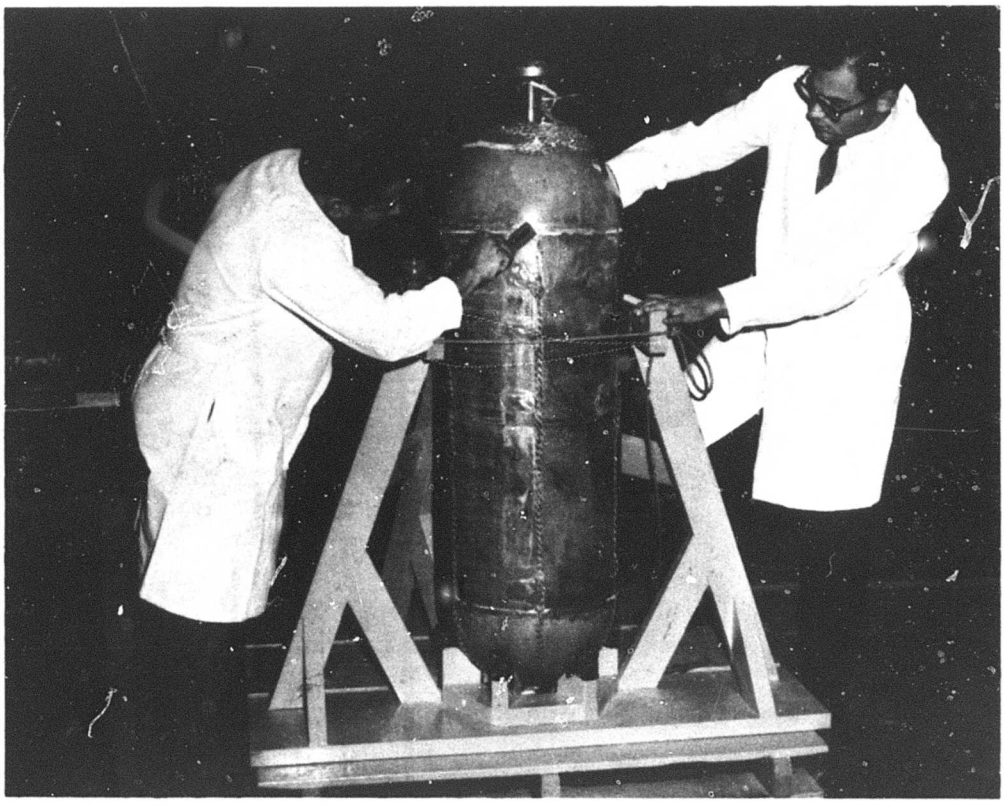

Figure 6. Hemispherical closure being epoxy-bonded to cylinder.

Figure 7. Beveled end closure with differential transformer ready for bonding.

After assembly, each specimen was coated with a waterproofing epoxy so that the concrete would remain dry during pressure testing.

Instrumentation

Specimens 1 through 8 were instrumented with electrical resistance strain gages (BLH A-5-1-S6) located on the exterior surface in the hoop direction only. Specimens 9 through 12 were not instrumented. Figures 8 through 11 show the gage layout for the free, pinned, beveled, and fixed end conditions, respectively. The gage layouts for the specimens were similar in that they measured the hoop strains along two radially opposite lines parallel to the cylinder axis. The strains along these lines, designated A and B, show the influence of the end closure on the radial displacement relative to the distance from the closure. Six gages were placed around the cylinder at locations 2, 8, and 16 inches from the edge of the closure. These strain measurements around the circumference show cylinder out-of-roundness and the development of flat spots.

The strain gages were attached to the cylinder with an epoxy (EPY 150) and were waterproofed with a microcrystalline wax.

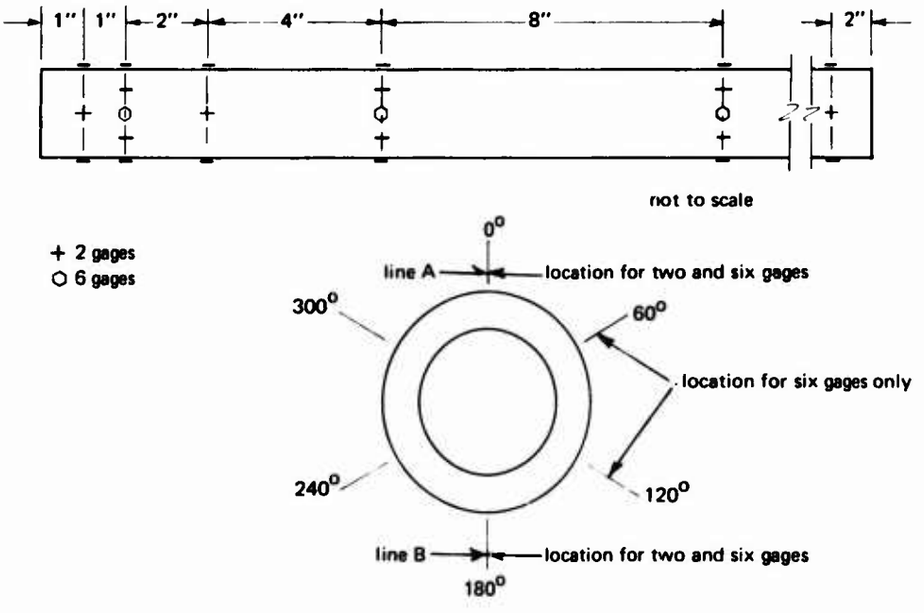

Figure 8. Strain gage layout, specimens 1 and 2 (free end closures).

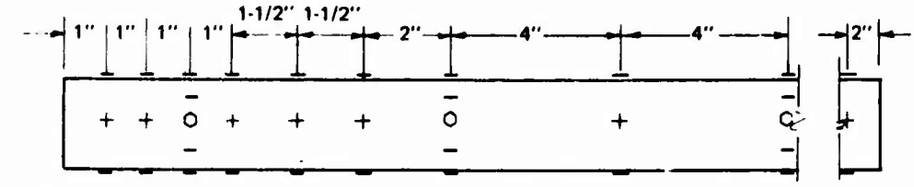

Figure 9. Strain gage layout, specimens 3 and 4 (pinned end closures).

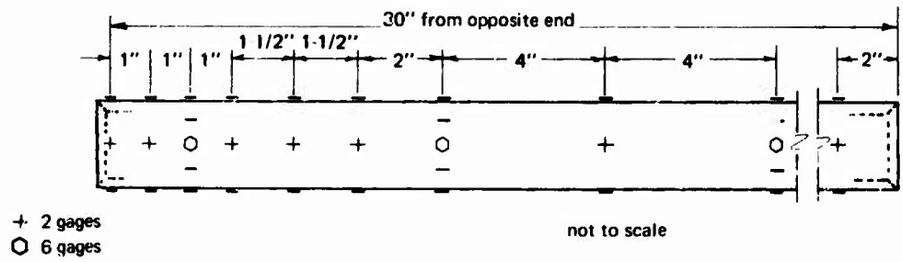

Figure 10. Strain gage layout, specimens 5 and 6 (beveled end closures).

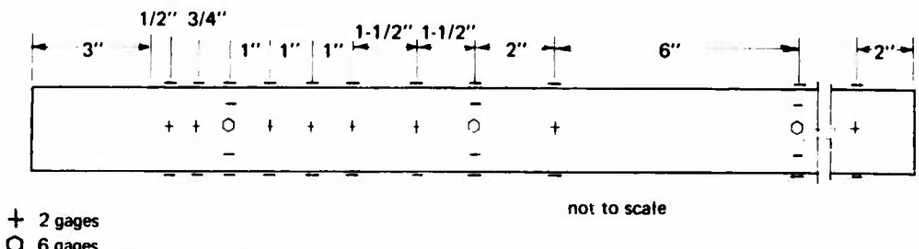

Figure 11. Strain gage layout, specimens 7 and 8 (fixed end closures).

A linear differential transformer was used on specimens 3 through 8 to measure the interior radial displacement of line A at a distance 1 to 3 inches from the closure. The transformer (pictured in Figure 7) was used principally to provide data for comparison with the exterior displacements measured by strain gages. The transformer was connected to a bracket having a highly magnetized base plate which rigidly adhered to the steel end closure.

During assembly of the specimens the strain gage lead wires were run down the exterior of the cylinder, through a penetration in the lower hemisphere to the interior, then out of the cylinder through the upper end closure. The lower penetration was potted with epoxy. The lead wire from the differential transformer was brought out of the cylinder through the upper end closure.

During the pressure test, strain gage readings were recorded on a Datran I Strain Indicator and Recorder System. The measurements were within an accuracy of ±10μin./in. The differential transformer was monitored with a N-type strain indicator previously used to calibrate the transformer.

Test Procedure

All specimens were tested in the 72-inch-ID x 160-inch-long hydrostatic pressure vessel at NCEL. After the specimen was attached to the head of the vessel (Figure 12), the cylinder was partially filled with water to reduce the violent forces created by implosion. The strain gage and differential transformer lead wires were brought out of the vessel through the connection in the vessel head.

The specimen was then loaded under hydrostatic pressure at a rate of 100 psi per minute between data recordings until implosion occurred. Strain and transformer readings were taken every 100 psi. The time required to record the data was approximately 30 seconds, during which the pressure loading was held constant.

After implosion the specimen was removed from the vessel and inspected.

TEST RESULTS

Failed Specimens

The failure mode of specimens 1, 2, 3, 4, 5, 6, and 8 was a bearing shear type failure at the joint between the concrete hemispherical end closure and the cylinder (Figure 13). The shear plane was at approximately

a 45-degree angle and ranged between one-sixth to one-half of the circumference at the joint. The failure plane was not limited to the cylinder section but ran continuously through the cylinder, epoxy joint, and hemisphere. In every case hemisphere fragments remained firmly bonded to the cylinder.

Implosion of specimen 7 was caused by a local failure of the concrete hemisphere (Figure 14). The sides of this local failure showed the typical concrete compression failure observed in previous studies of concrete spheres.[3,4]

The failure mode of specimens 9, 10, 11, and 12 was a concrete compression type failure of the cylinder (Figures 15 and 16 show typical examples). The shear plane angle was between 30 and 45 degrees tangent to the exterior surface and ranged between the bottom and top of the hole (Figure 15). The failure plane was located between 4 and 12 inches from the edge of the steel plate end closures. This failure mode was identical to that observed by Haynes and Ross[1] on 2-inch-thick cylinders capped with 2-inch-thick hemispheres.

Forces created by implosion caused the bond to break between the cylinder and the pinned and beveled end closures. The fixed end closures remained attached to the cylinders. The steel plates showed no damage or dimensional change after the test.

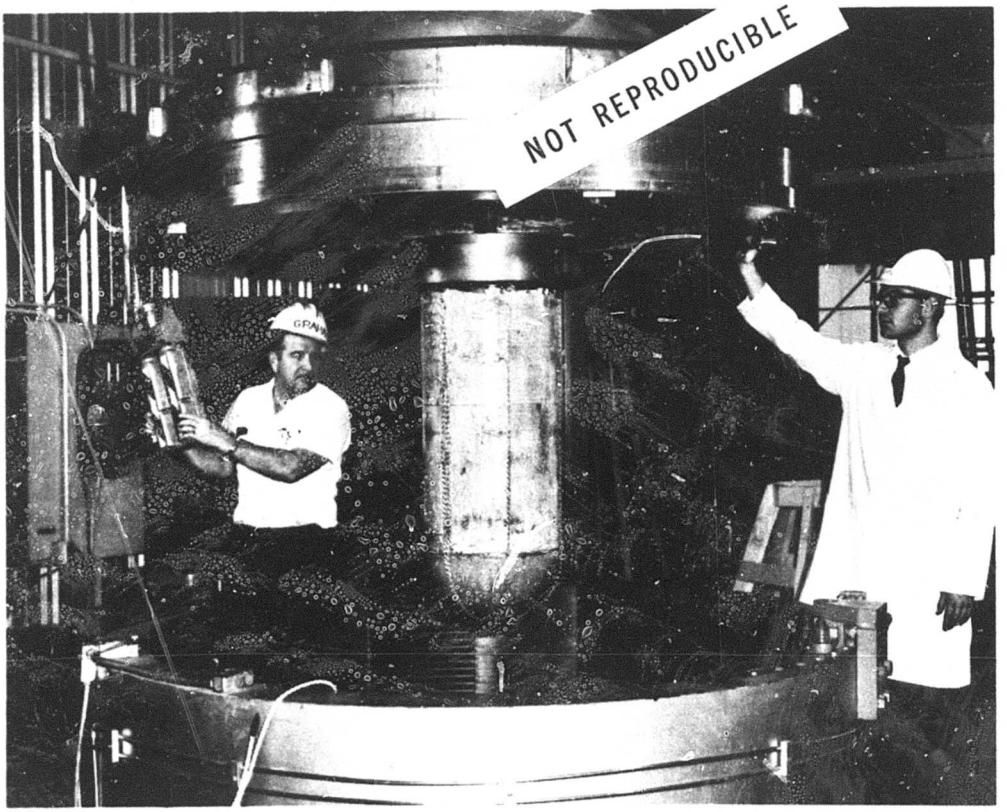

Figure 12. Cylinder with fixed end closure being lowered into pressure vessel for hydrostatic test.

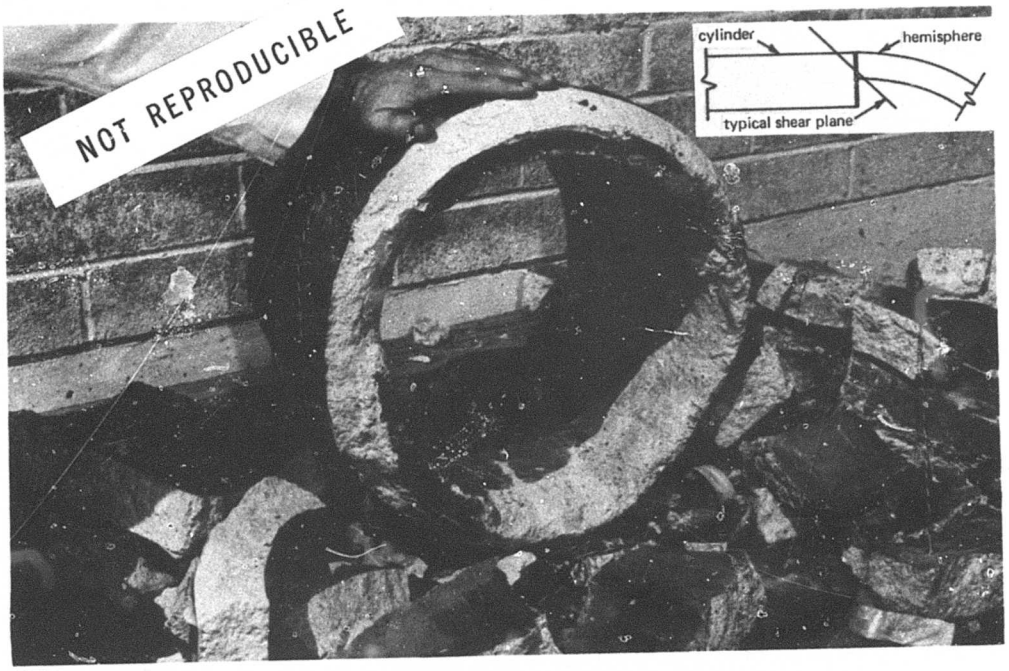

Figure 13. Bearing shear failure at cylinder edge for specimen 1.

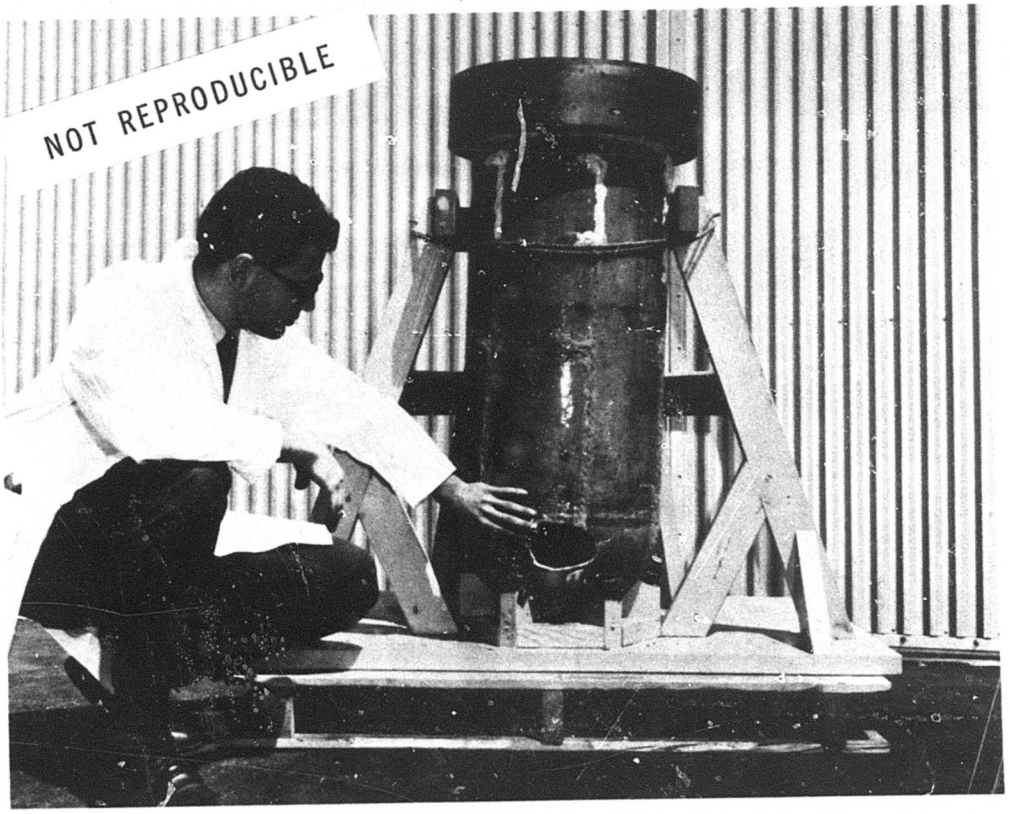

Figure 14. Local failure of hemispherical end on specimen 7.

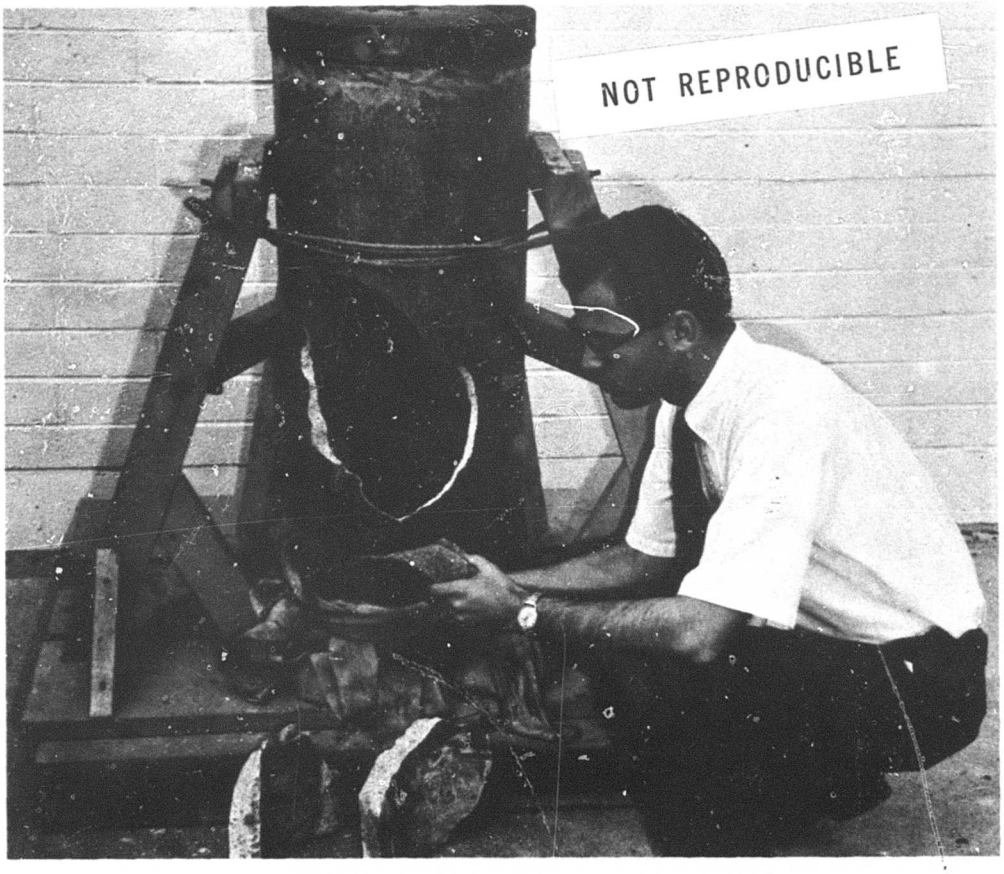

Figure 15. Failure of cylinder section for specimen 9.

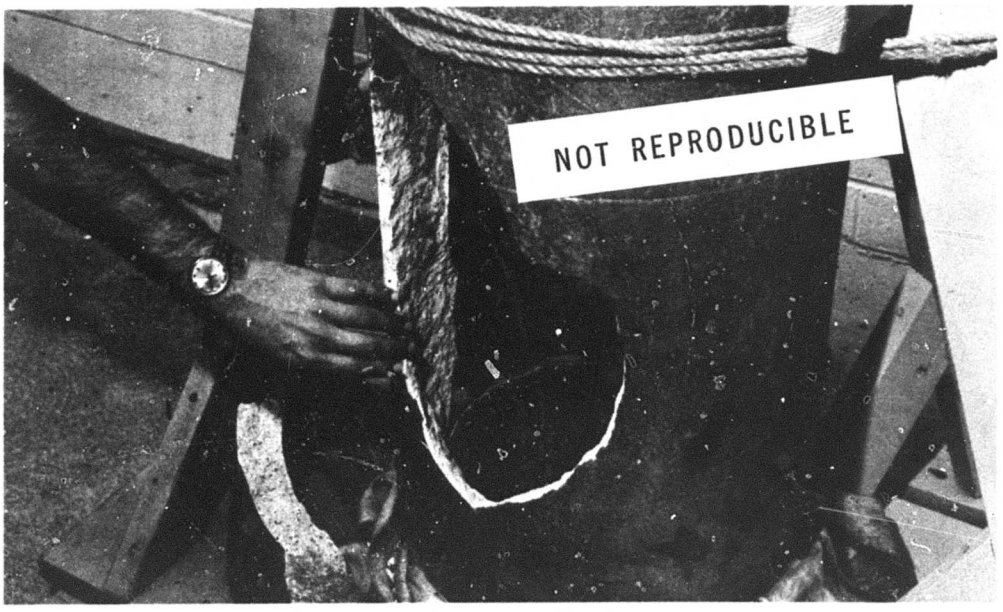

Figure 16. Close up of failure plane of specimen 9.

Implosion Data

Implosion test results are presented in Table 2. The implosion behavior of the specimens was compared using the ratio of implosion pressure to concrete strength, P_{im}/f'_c. This ratio accounts for differences in implosion pressures caused by variation of concrete strength.

Table 2. Implosion Test Data

Specimen No.	End Condition	Implosion Pressure, P_{im} (psi)	Concrete Strength, f'_c[a]	P_{im}/f'_c
1	free	1,800	7,860	0.229
2	free	2,195	9,800	0.224
3	pinned	2,300	9,420	0.244
4	pinned	2,355	9,270	0.254
5	beveled	1,145	5,940	0.193
6	beveled	1,350	5,910	0.229
7	fixed	2,275	9,100	0.250
8	fixed	2,190	9,260	0.236
9	beveled	2,655	10,480	0.253
10	beveled	2,480	10,640	0.233
11	fixed	2,835	8,700	0.326
12	fixed	2,435	9,580	0.254
5[b]	2-in.-thick hemisphere	2,600	10,120	0.257
6[b]	2-in.-thick hemisphere	2,800	10,120	0.277

[a] The concrete strength is an average of six 3 x 6-inch control cylinders made from the same concrete used to cast the cylinder section.

[b] Data from experiments by Haynes and Ross on concrete cylinders with L/D_o = 2.0 and with 16-inch-OD x 2-inch-wall-thickness hemispherical closures on each end.[1]

Strain Data

Figures 17 through 24 present the exterior hoop strains of lines A and B versus the distance from the edge of the end closure for specimens 1 through 8, respectively. So that the various specimens could be easily compared, the strains were plotted at two pressure levels corresponding to two ratios of applied pressure to concrete strength of the cylinder section, $P/f'_c = 0.10$ and $P/f'_c = 0.20$. The measured "distance from edge of closure" for specimens 1 and 2 was the distance from the hemisphere–cylinder joint, for specimens 3 and 4 it was from the bearing point of the pinned end closure, for specimens 5 and 6 it was from the interior edge of the bevel of the cylinder section, and for specimens 7 and 8 it was from the edge of the interior face of the fixed end closure.

Figures 25 through 32 present the exterior hoop strains around the circumference at 2, 8, and 16 inches from the edge of the closure versus the degrees around the circumference for specimens 1 through 8, respectively. As before, the strains were plotted at two ratios of applied pressure to concrete strength. Line A was designated as the 0^o point, and the angle around the circumference increased clockwise as one would view the cylinder from the end with the steel plate closure.

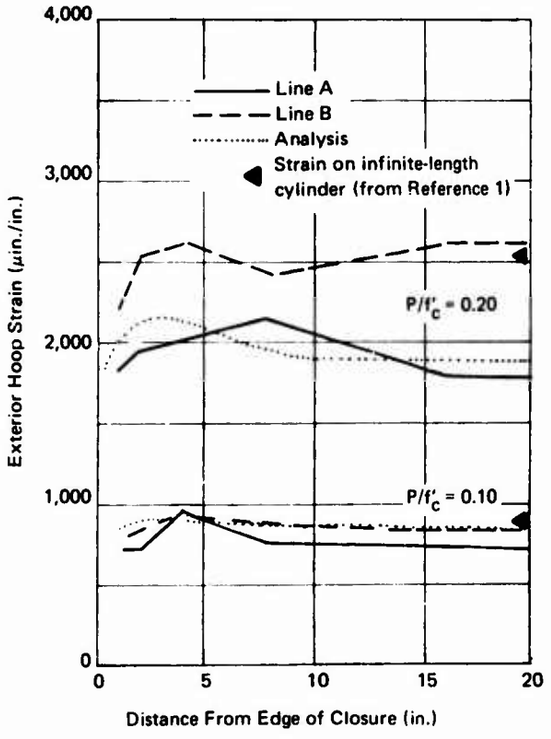

Figure 17. Strain along length of specimen 1.

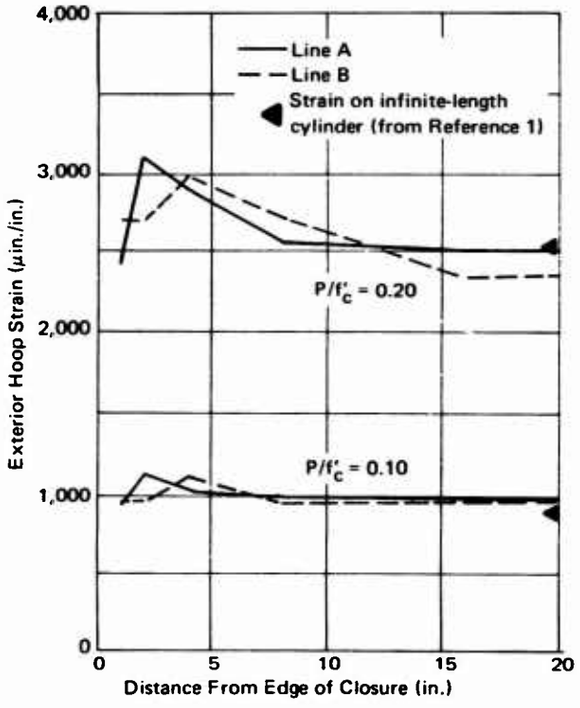

Figure 18. Strain along length of specimen 2.

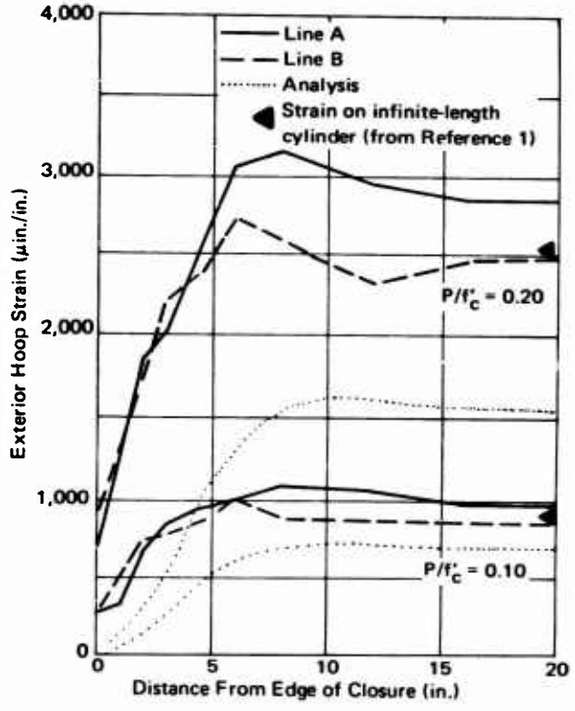

Figure 19. Strain along length of specimen 3.

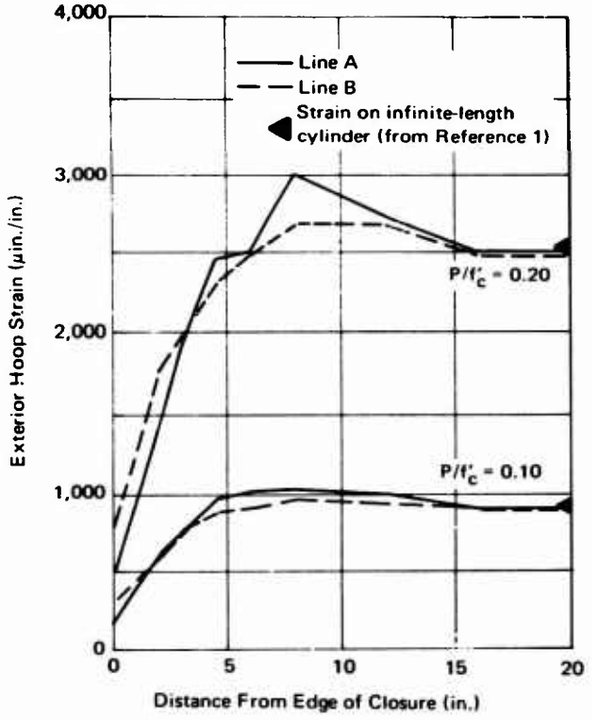

Figure 20. Strain along length of specimen 4.

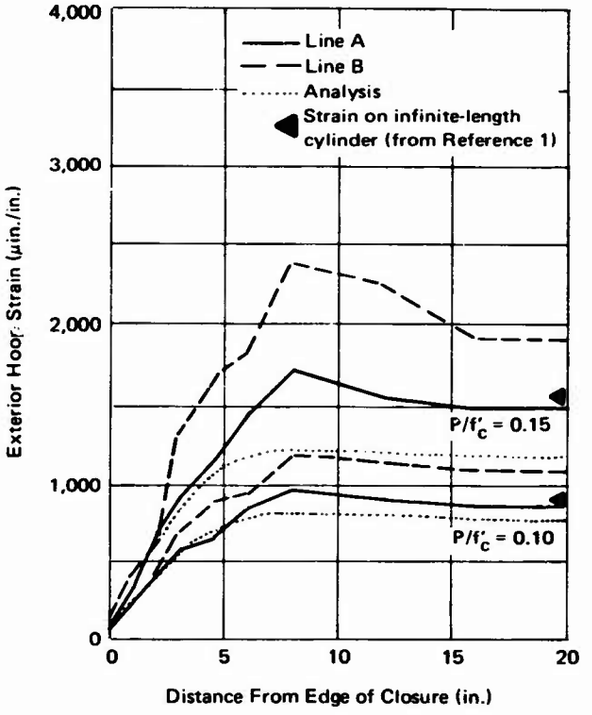

Figure 21. Strain along length of specimen 5.

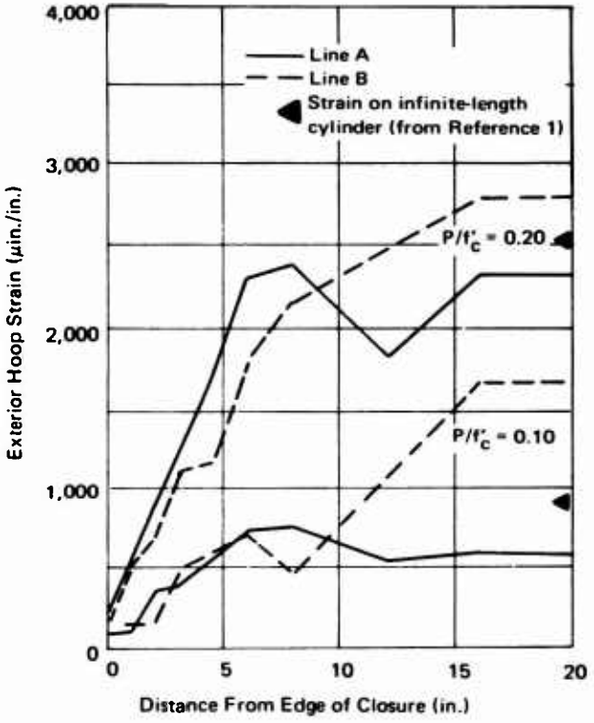

Figure 22. Strain along length of specimen 6.

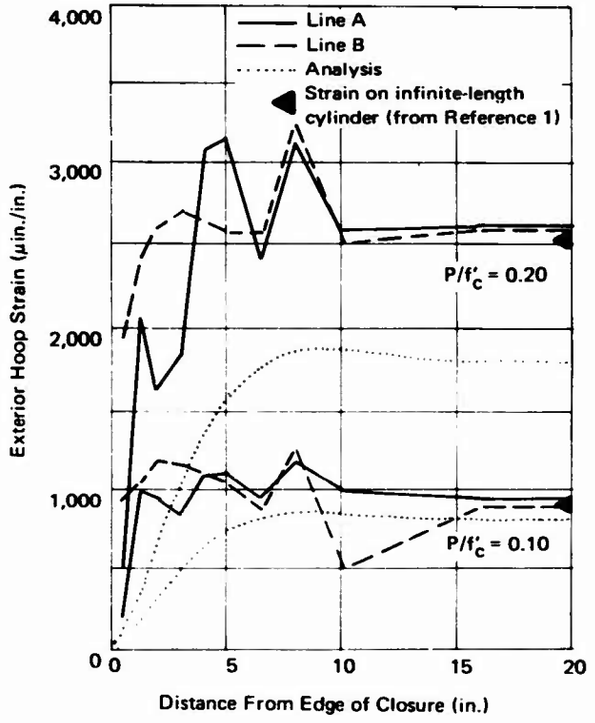

Figure 23. Strain along length of specimen 7.

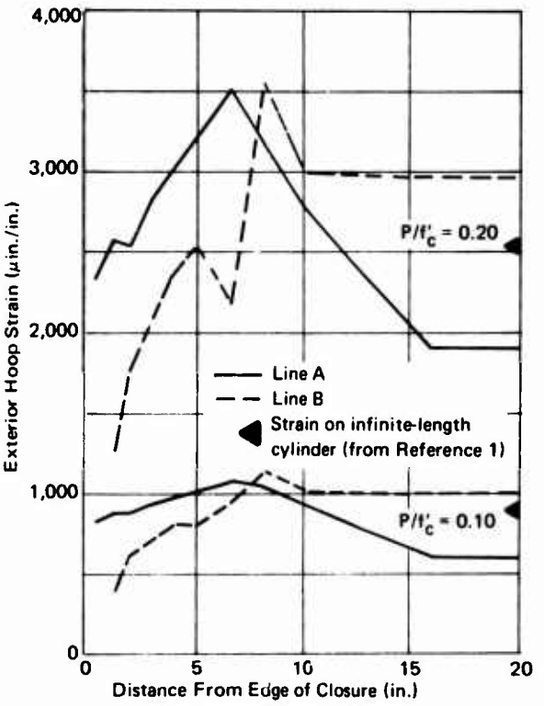

Figure 24. Strain along length of specimen 8.

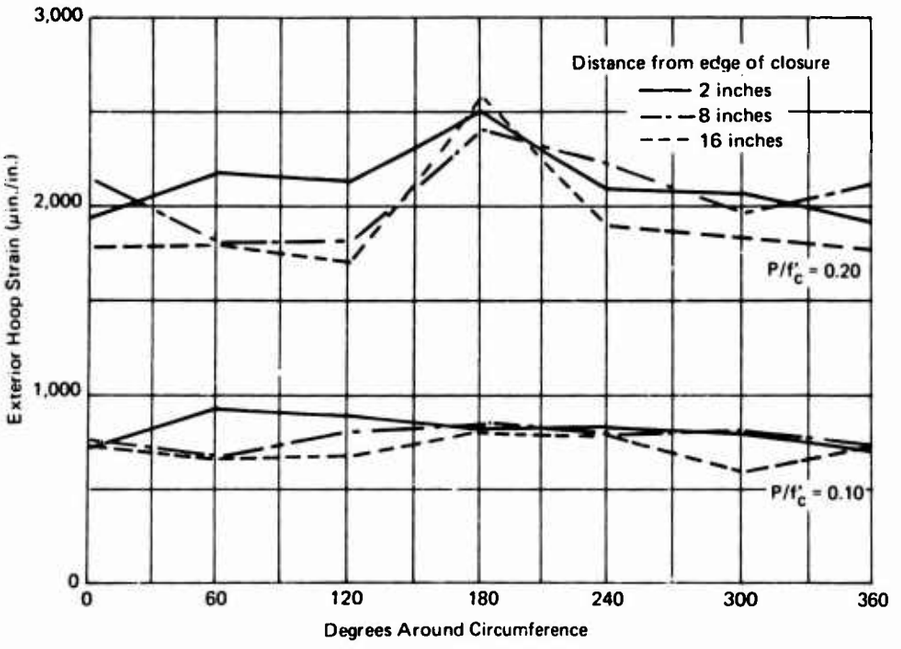

Figure 25. Circumferential strain, specimen 1.

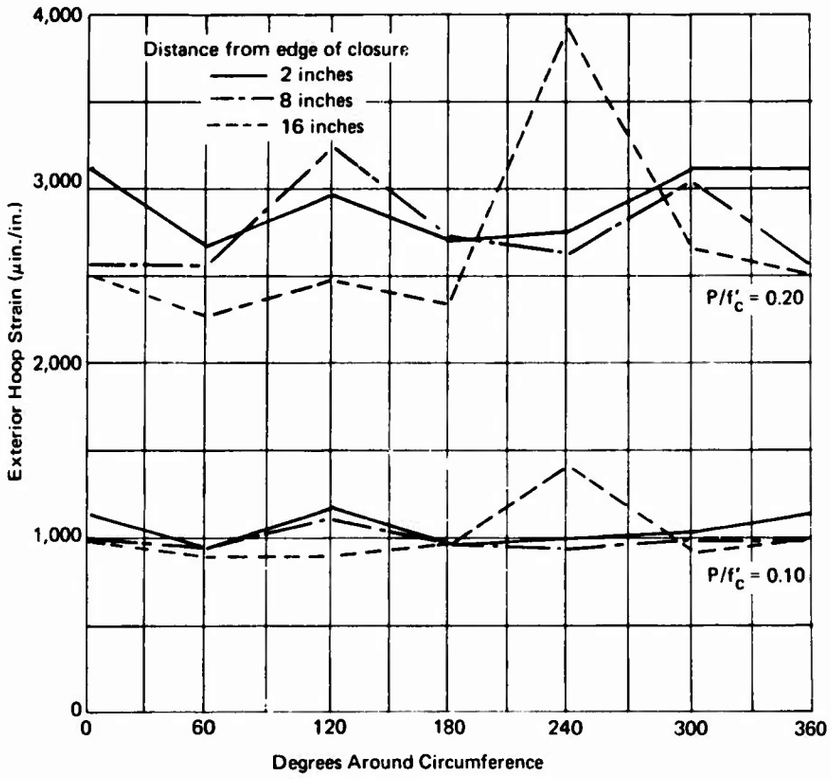

Figure 26. Circumferential strain, specimen 2.

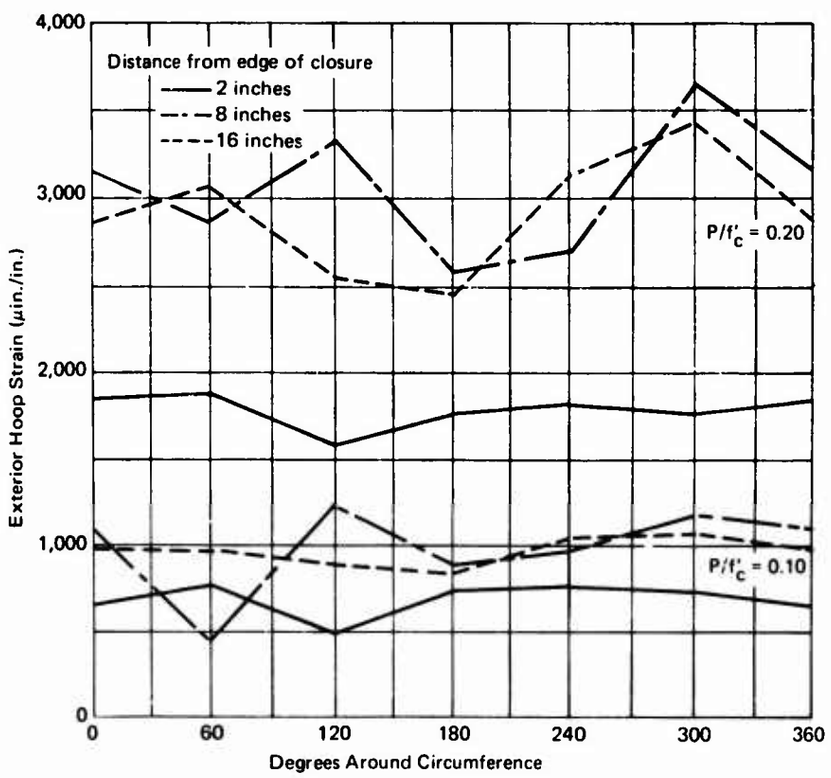

Figure 27. Circumferential strain, specimen 3.

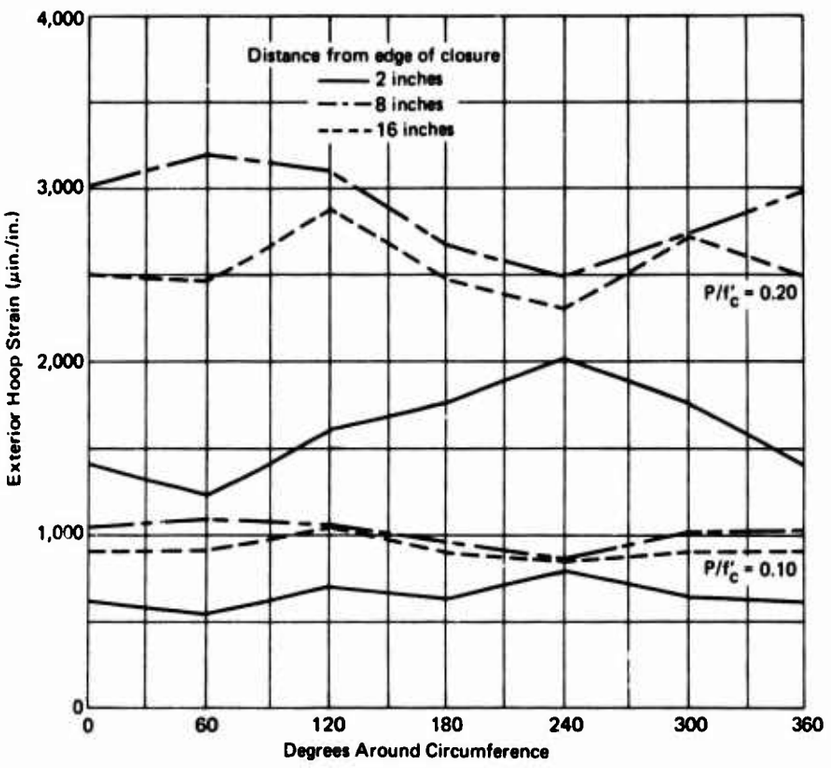

Figure 28. Circumferential strain, specimen 4.

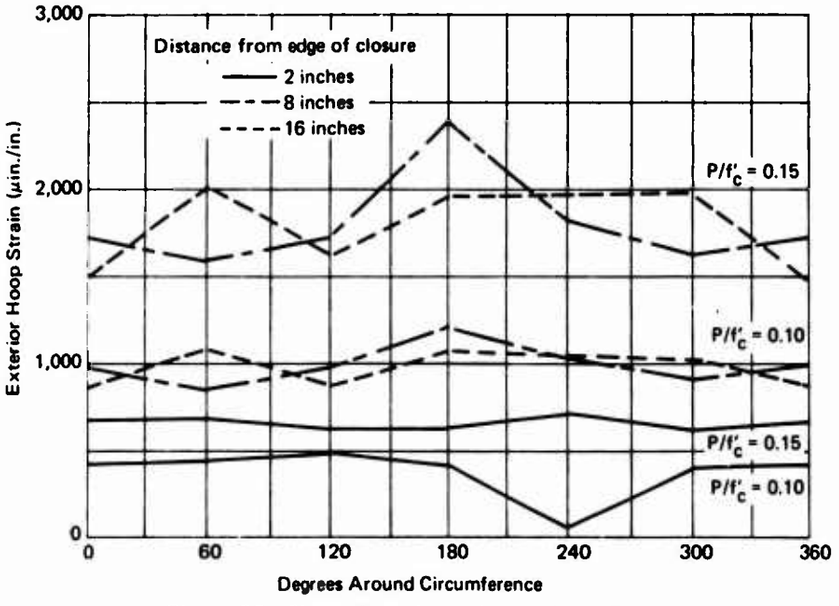

Figure 29. Circumferential strain, specimen 5.

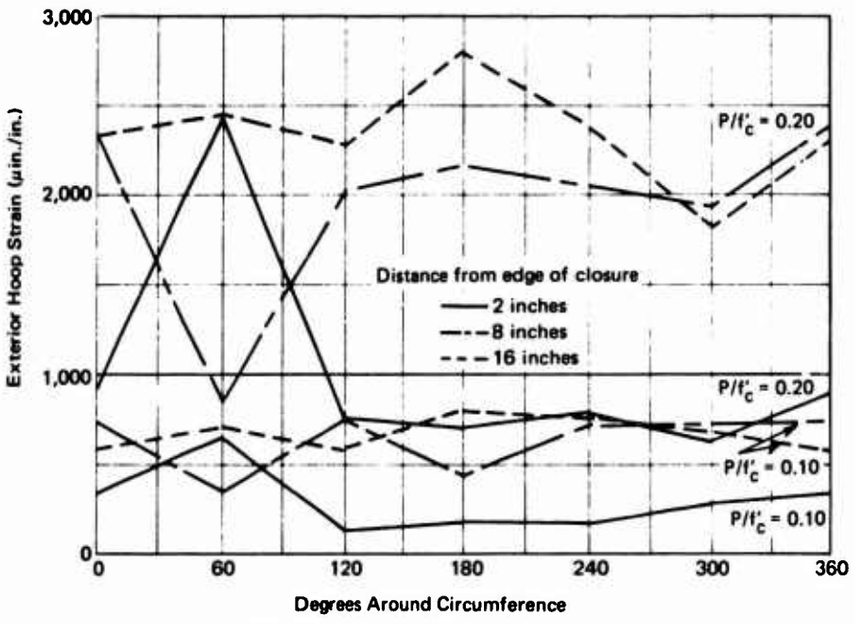

Figure 30. Circumferential strain, specimen 6.

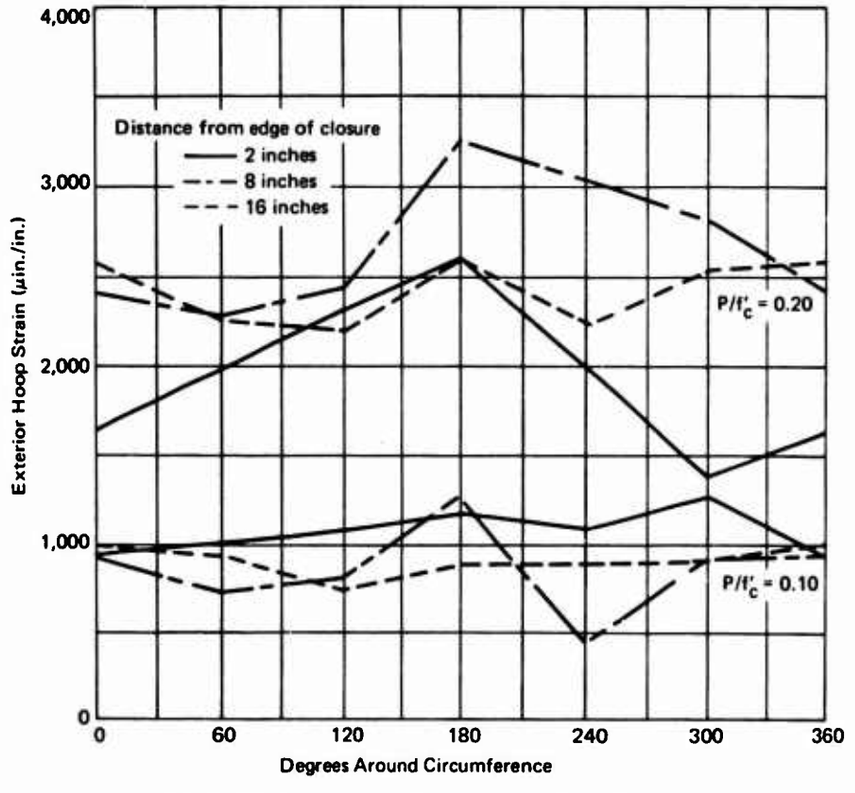

Figure 31. Circumferential strain, specimen 7.

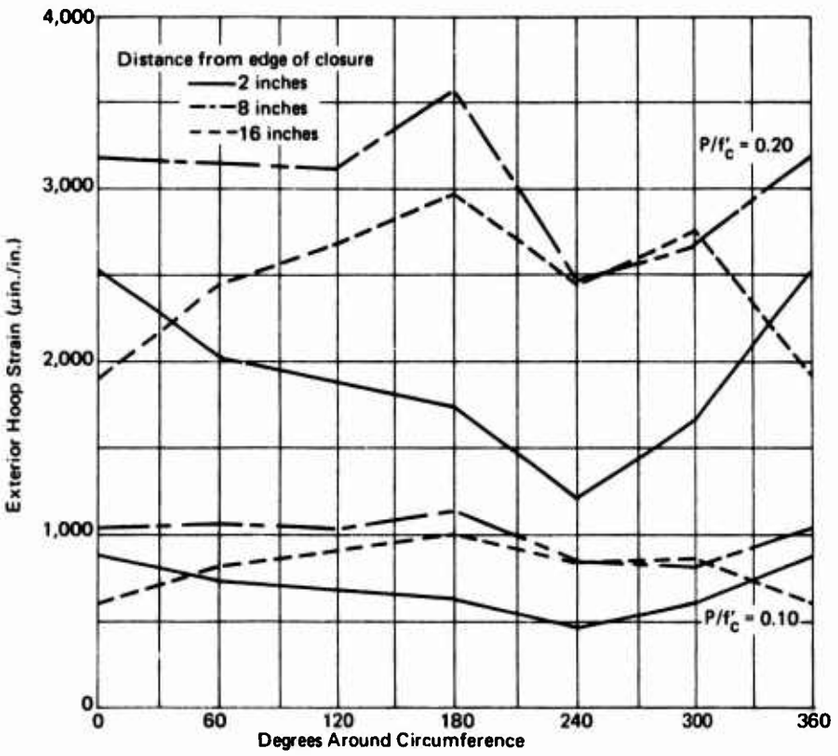

Figure 32. Circumferential strain, specimen 8.

Linear Differential Transformer Data

Differential transformers were not used on specimens 1 and 2. The transformers on specimens 5 and 7 were inoperable because when the closures were epoxied to the hulls some epoxy had flowed down the inner side of the hulls and bonded the rod to the coil. Figure 33 shows P/f'_c plotted versus the inside radial deflection and calculated interior hoop strain for specimens 3, 4, 6, and 8.

Finite Element Analysis

The finite element technique was used to analyze specimens 1, 3, 5, and 7. The concrete strengths of each cylinder and the bilinear stress–strain curves for the concretes were used in the analysis (the bilinear curve is discussed in Appendix A). The results of the analysis are plotted along with the experimental data on Figures 17, 19, 21, and 23 for the respective specimens. It was assumed that there was no initial out-of-roundness in any cylinder and therefore no development of a flat spot as load was applied. In the analysis, the mechanical properties of the cylinder also were used for

the hemisphere end. The connections between the cylinder sections and the steel plates were assumed to be "perfect" connections; that is, there was no discontinuity between the cylinder and the "pin" for specimen 3, the beveled plate was symmetric with a uniform epoxy joint for specimen 5, and full fixity occurred at the joint between the cylinder and the plate for specimen 7.

The exterior radial displacements were calculated for specimens 3, 5, and 7 at the positions where the differential transformers were located. These data are plotted in Figure 33 along with the experimental results.

DISCUSSION

Implosion Behavior

Lamé's elastic thick-wall theory was used to predict the implosion pressure of the cylindrical hulls by assuming that failure of the cylinder occurred when the interior hoop stress reached the ultimate concrete strength. The Lamé expression is

$$P_{im} = f'_c\left(\frac{r_o^2 - r_i^2}{2r_o^2}\right) \qquad (1)$$

where P_{im} = implosion pressure (psi)

f'_c = ultimate uniaxial concrete strength (psi)

r_i = interior radius, which is the location under consideration (in.)

r_o = exterior radius (in.)

When the dimensions of the specimens are substituted in Equation 1, the resulting implosion pressure is

$$P_{im} = 0.219\, f'_c \qquad (2)$$

or the ratio of implosion pressure to concrete strength (P_{im}/f'_c) is 0.219.

All specimens except specimen 5 imploded at a pressure higher than that predicted by Lamé's equation. The P_{im}/f'_c ratio for specimen 5 was 12% lower than 0.219. The average P_{im}/f'_c ratio for specimens 1 through 8 was

0.232, for specimens 9 through 12 it was 0.266, and the average for all specimens was 0.244. Haynes and Ross[1] found that the P_{im}/f'_c ratio for cylinders with a L/D_o ratio greater than 2.0 ranged between 0.220 and 0.277 with an average of 0.250.

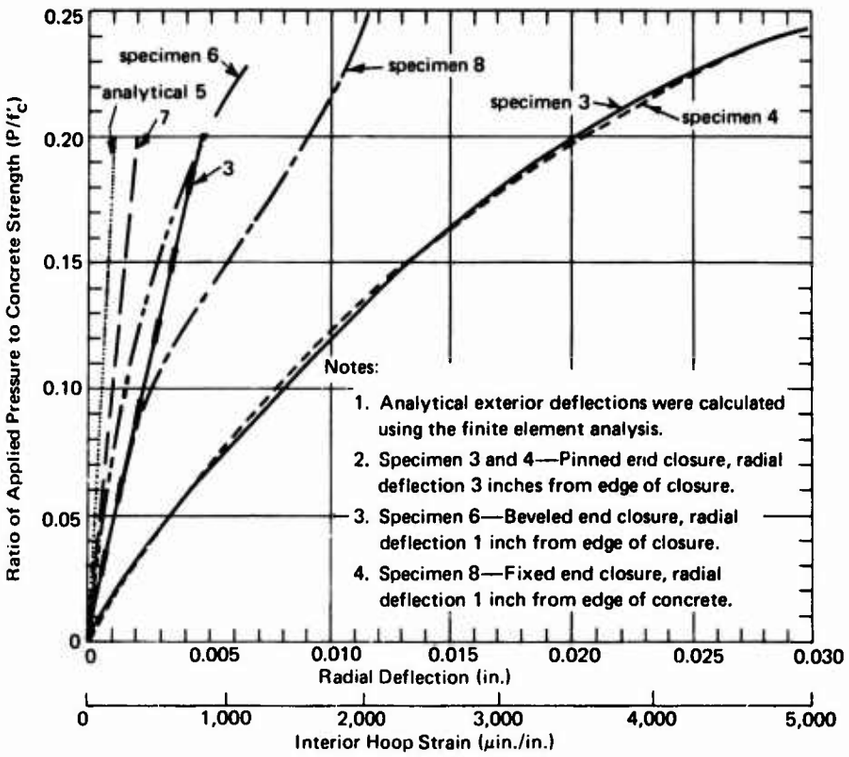

Figure 33. Linear differential transformer data: radial deflection and interior hoop strain near end closure on line A.

Therefore the specimens of this study generally failed at pressures between those which caused failure of "infinitely" long cylinders and those predicted by elastic theory.

The mode of failure observed by Haynes and Ross[1] was that a section of the cylinder imploded by forming a shear plane approximately parallel to the cylinder axis. An identical failure mode was observed in specimens 9 through 12. The shear plane in the latter specimens occurred near the hemispherical closure rather than near the plate closure. Although both closures induced a strain increase about 8 inches from the edge, the stiffer closure apparently restrained the cylinder more than did the hemisphere, allowing the concrete to collapse near the hemispherical closure. Except for sphere 7, specimens 1 through 8 failed by concrete shear created by high bearing stresses on the edge of the cylinders. This mode of failure caused

specimens 1 through 6 and specimen 8 to implode at pressures an average 15% lower than implosion pressures of specimens 9 through 12 and an average 8% lower than those recorded in the previous study. Table 3 lists the end bearing stresses produced by the hemispherical closure, the concrete strength of the cylinder section, and the percentage difference. The bearing stress at implosion was essentially equal to the concrete strength. This indicated that the specimens failed because the bearing stress reached the ultimate concrete strength.

Table 3. Bearing Stresses Produced by 1-Inch-Thick Hemispherical Closures

Specimen No.	Calculated Bearing Stress at Implosion	Concrete Strength of Cylinder Section, f'_c (psi)	Difference Between Bearing Stress and Concrete Strength[a] (%)
1	7,680	7,860	-2.3
2	9,380	9,800	-4.3
3	9,810	9,420	+4.1
4	10,050	9,270	+8.4
5	4,880	5,940	-17.8
6	5,760	5,910	-2.5
7	9,700	9,100	+6.6
8	9,350	9,260	+1.0

[a] $\text{Difference} = \dfrac{\text{bearing stress} - f'_c}{f'_c} \times 100.$

Strain Behavior

The strains observed in these experiments were exterior strains only. It is logical to assume that the locations of maximum exterior and interior hoop strains were the same and that the structural response at the exterior was similar to that at the interior. Elastic thick-wall theory predicted that the interior strain would be 33% greater than the exterior strain; Haynes and Ross found that the interior strains were between 33% and 50% greater.[1]

Therefore, in reviewing the graphs of "strain versus distance from edge of closure" (Figures 17 through 24), the reader should recognize that the *maximum* strains were more than one-third greater than those recorded.

Strain Variation Along Cylinder Length. The influence of the end closure on the strain along the cylinder length is reviewed for each specimen in Appendix C. Generally, the pinned, beveled, and fixed closures produced similar cylinder behavior: nearly complete restraint against radial deflection at the cylinder end, a maximum deflection at a distance approximately 8 inches from the edge of the closure, and significant shear strain in the region between the end closure and the point of maximum deflection. The influence of all closures was limited to a distance of approximately 16 inches from the end.

This behavior was similar to that observed by Haynes and Ross.[1] Their results of "strain versus distance from edge of closures" are shown in Figure 34. On all the various length cylinders, the closures were 2-inch-thick hemispheres. Hoop strains were measured from the closure edge to the midlength of the cylinder. The response of cylinders with $L/D_o = 1$ and $L/D_o = 4$ was similar to that of specimens 3 through 8: restrained deflection near the closure, increased deflection between 4 and 8 inches from the edge, and more uniform deflection beyond 16 inches for the cylinder with $L/D_o = 4$.

The cylinder with $L/D_o = 8$ showed that beyond 16 inches from the edge the strains were relatively uniform. These strains are indicative of those of an infinitely long cylinder. The strain values between 16 inches and 64 inches from the edge were averaged at the two pressure levels ($P/f'_c = 0.10$ and 0.20) on the cylinder with $L/D_o = 8$. The averages represent a base line strain value for an infinitely long cylinder. These averages were plotted on Figures 17 through 24 as a comparison for the experimental strains found at 16 inches from the closure. In general these base line values were between the strains recorded on line A and line B at 16 inches from the edge or were nearly equal to one of those strain values. This agreement shows that the strains obtained at 16 inches from the closure on specimens 1 through 8 were representative of the strains of an infinitely long cylinder, and the agreement verifies that the influence of the closure is limited to a distance of one outside diameter from the edge of the closure.

The maximum radial deflection was a result of a longitudinal moment created by the bearing load of the end closure on the cylinder in conjunction with the uniform cylinder deflection. As pressure loading was applied and the concrete cylinder deflected radially, a moment arm was developed between the restrained end of the cylinder and portions farther from the end (Figure 35). The longitudinal moment thus created caused an increased radial deflection approximately 8 inches from the edge of the closure.

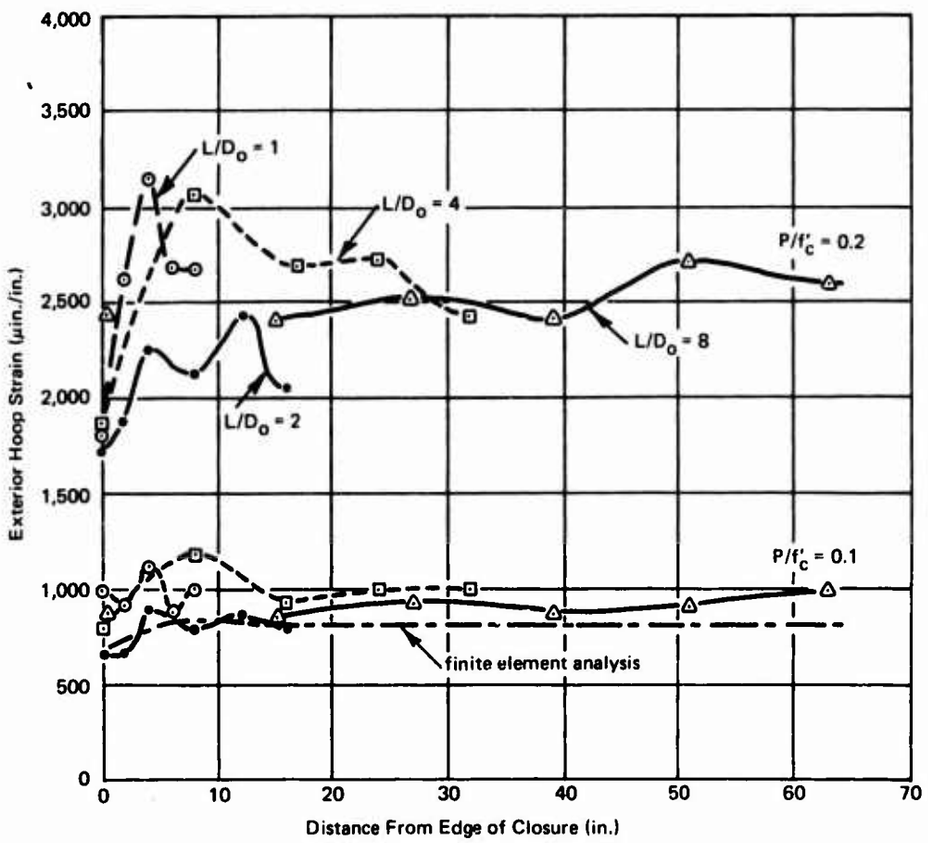

Figure 34. Comparison of exterior hoop strain behavior for cylinders of different lengths. (After Reference 1.)

A relative measure of this maximum deflection is the ratio of the maximum hoop strain and the strain at the midlength of the cylinder (16 inches from the edge). This ratio, termed strain magnification ratio, was calculated for the first eight specimens using strain values of both line A and line B, for the four models analyzed by the finite element method, and for the cylinder with $L/D_o = 4$ tested by Haynes and Ross.[1] The strain magnification ratios are listed in Table 4. A high ratio implies that the end-closure condition caused a larger strain (radial deflection) in the cylinder than that found on a cylinder of infinite length; a low value of the ratio means that the end-closure condition had little effect on the maximum strain behavior of the cylinder.

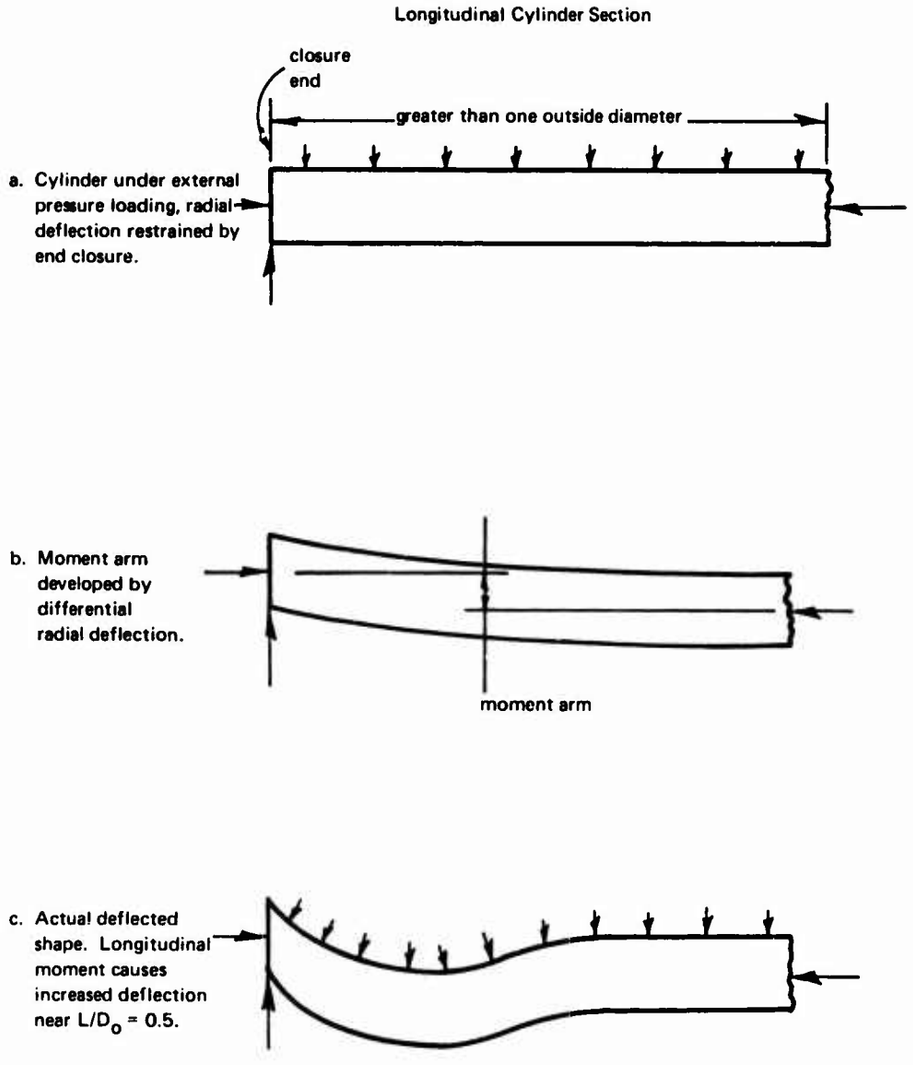

Figure 35. Schematic diagram of cylindrical hull deflection when radial deflection is restrained at one end.

Table 4. Strain Magnification Ratio at P/f'_c = 0.10 and 0.20[a]

Specimen and Closure Type	Strain Magnification Ratio at—					
	P/f'_c = 0.10			P/f'_c = 0.20		
	Line A	Line B	Analysis	Line A	Line B	Analysis
1, free	0.24	0.12	0.10	0.19	0.00	0.14
2, free	0.14	0.17	–	0.24	0.27	–
3, pinned	0.11	0.16	0.03	0.12	0.11	0.03
4, pinned	0.14	0.07	–	0.20	0.08	–
5, beveled	0.13	0.08	0.04	0.15[b]	0.24[b]	0.04
6, beveled	0.27	0.00	–	0.03	0.00	–
7, fixed	0.24	0.40	0.02	0.21	0.25	0.03
8, fixed	0.75	0.12	–	0.32	0.21	–
Cylinder with L/D_o = 4 of Reference 1	0.24	–	–	0.14	–	–

[a] Strain ratio = $\frac{\text{maximum strain} - \text{strain at 16 inches}}{\text{strain at 16 inches}}$.

[b] Ratio at P/f'_c = 0.15.

The experiments showed that all cylinders had a magnification ratio greater than 10%, which indicated that all end closures produced a significant strain increase. Specimens 1 through 6 and the cylinder with L/D_o = 4 of Reference 1 had similar ratios; the free, pinned, beveled, and 2-inch-thick hemispherical closures caused approximately the same strain increase. Specimens 7 and 8, with the fixed end closure, had greater strain magnification ratios. It is believed that the moment induced by the fixed end closure in conjunction with the longitudinal moment created by the end bearing of the closure produced the larger maximum strain increase.

Strain Variation Around Cylinder Circumference. In general the differences in circumferential strains in a single specimen were as great as the strain differences caused by varying the end closures between specimens. Apparently the end closures did not prevent flat spot development near the cylinder ends; all sections of the cylinders developed similar out-of-round conditions.

The circumferential strains at 2, 8, and 16 inches from the closure showed the out-of-roundness and the unsymmetric response of the eight cylinders. The circumferential strain data in Figures 25 through 32 have been reduced to quantitative parameters at two pressure levels (P/f'_c = 0.10 and 0.20) and are listed in Table D-1 of Appendix D. A nondimensional "roundness ratio" was computed as the difference between the maximum and mean strains divided by the mean strain. This ratio was determined at locations 2, 8, and 16 inches away from the edge of the closure and at pressure levels P/f'_c = 0.10 and 0.20. The roundness ratios are listed in Table 5.

Table 5. Roundness Ratio at P/f'_c = 0.10 and 0.20[a]

Specimen No.	Roundness Ratio at—					
	P/f'_c = 0.10			P/f'_c = 0.20		
	2 Inches From Closure	8 Inches From Closure	16 Inches From Closure	2 Inches From Closure	8 Inches From Closure	16 Inches From Closure
1	0.7	0.09	0.16	0.16	0.16	0.33
2	0.13	0.13	0.38	0.08	0.16	0.44
3	0.12	0.27	0.07	0.04	0.20	0.18
4	0.22	0.08	0.04	0.25	0.11	0.12
5	0.35	0.22	0.09	0.09[b]	0.27[b]	0.15[b]
6	1.27	0.21	0.08	1.36	0.27	0.20
7	0.17	0.47	0.11	0.32	0.20	0.09
8	0.31	0.16	0.19	0.38	0.18	0.17

[a] Roundness ratio = $\frac{\text{maximum circumferential strain - mean circumferential strain}}{\text{mean circumferential strain}}$.

[b] Ratio at P/f'_c = 0.15.

A high roundness ratio indicated that the cylinder was deflecting considerably more in one area than in another, that the cylinder was out-of-round, and that a flat spot was developing. A lower ratio value showed that the cylinder was maintaining uniform curvature and equal deflection around the circumference.

The roundness ratios listed in Table 5 indicated that out-of-roundness was random. In general the cylinders were not restrained from developing a flat spot near the closure; out-of-roundness at the midlength was not significantly different from that near the closure.

A comparison between the nondimensional roundness ratios and strain magnification ratios showed that out-of-roundness produced as much strain deviation as that produced by the end-closure condition. The end closures induced higher absolute strain values near the cylinder end, but these strain increases did not appear to alter the flat spot development.

A further discussion of minor differences in circumferential strain is continued in Appendix D.

Comparison Between Experimental and Analytical Results

The finite element analysis predicted behavior similar to that observed, except that the calculated strains were between 0% and 130% less than those recorded. Figure 36 compares the experimental and analytical results by showing the maximum strain occurring between the closure and 16 inches from the closure and the strain at 16 inches from the closure (for the experimental results, the mean strain listed in Table D-1 is shown).

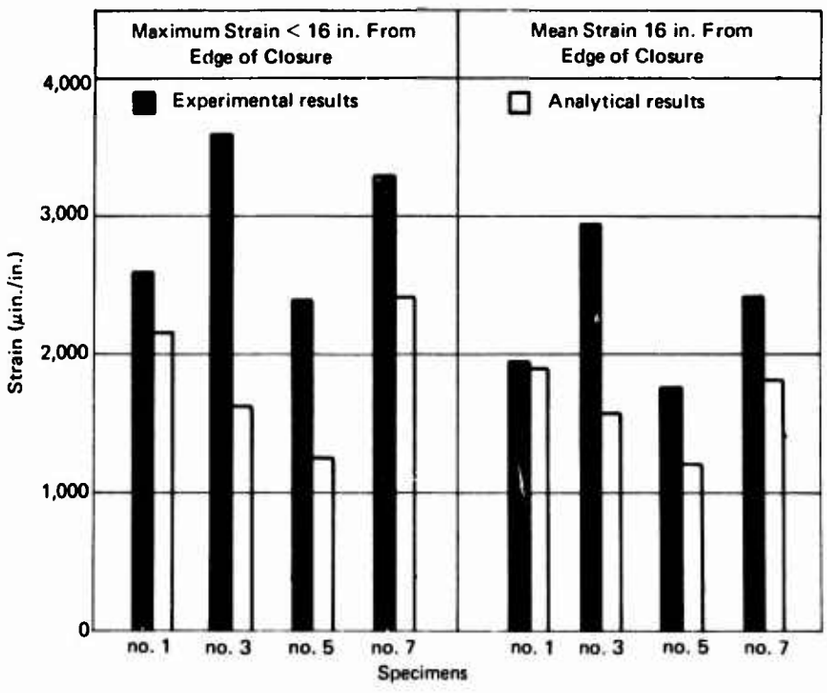

Figure 36. Comparison of experimental and analytical strain results at $P/f'_c = 0.20$.

The analysis was closest for the cylinder with the 1-inch-wall-thickness hemispherical closures at both ends, because no abrupt discontinuity in radial stiffness was introduced. Where more rigid end-closure restraints were introduced, the actual response of each finite element along the cylinder length was different from that of its neighboring element because of the nonlinearity of concrete and because of the influence of triaxial loading on the concrete properties. This difference in response was particularly important near the closure. The bilinear stress–strain curve used in the analysis did not accurately account for these real differences in response between the elements.

To analyze the structures more accurately, the real concrete stress–strain curve should be used in the computer program. Nevertheless, the linear analysis does show the areas of stress concentration, which may aid the designer in selecting the closure which induces the least stress conditions.

For cylinders with metal plate end closures, the maximum radial deflection was found both analytically and experimentally at a distance about one-half the outside diameter from the closure edge.

FINDINGS

1. Variations in the stiffness of cylinder end closures did not significantly alter the short-term implosion pressures of concrete cylindrical hulls from those pressures determined by Haynes and Ross.[1]

2. By using the concrete strength (f'_c) as the failure stress, Lamé's elastic thick-wall theory predicted implosion pressures less than those of the models, which had a t/D_o = 0.125, by approximately 10%.

3. For specimens with a 1-inch-thick hemispherical end closure, implosion resulted from a high bearing stress produced at the joint between the 1-inch-thick hemisphere and the 2-inch-thick cylinder section.

4. For specimens with a 2-inch-thick hemispherical end closure, implosion resulted from a concrete compression failure in the cylinder at a distance approximately one-half the outside diameter from the hemispherical closure.

5. The pinned, beveled, and fixed end closures produced similar cylinder behavior. Maximum radial deflection occurred at a distance from the closure equal to about one-half the outside diameter, and a region of high shear strain existed between the end closure and the point of maximum deflection.

6. Cylinder out-of-roundness and flat spot development caused as much strain variation in a specimen as that produced by the different end-closure conditions.

7. The influence of the end closures was limited to a distance equal to one outside diameter from the edge of the closure.

8. A finite element analysis using a bilinear stress–strain curve for concrete predicted the general behavior of cylindrical hulls with various end closures, but the analysis yielded strain values less than the values observed.

SUMMARY

Variation of end-closure stiffness did not reduce the implosion pressure of cylindrical concrete hulls below the implosion pressure of a cylinder with a free end condition or below the implosion pressure predicted with Lamé's theory. However, rigid end closures produced a severe shear strain near the closure and a maximum radial deflection at a distance approximately one-half the outside diameter from the closure restraint. The influence of end-closure stiffness was limited to the region one outside diameter from the closure.

RECOMMENDATIONS

In designing cylinder end closures and cylindrical hulls, the following guidelines are recommended:

1. The bearing load of the end closure on the cylinder should be applied at the center of cylinder wall thickness.

2. The closure stiffness should be approximately the same as that of the cylinder to reduce the maximum strains and create a uniform strain condition along the length of the cylinder.

3. Penetrations in the cylindrical hull should not be placed in the high-shear area between the closure and one-half the diameter from the closure.

4. Lamé's equation for thick-walled cylinders (Equation 1) may be used for a conservative prediction of implosion pressure for cylinders with $t/D_o = 0.125$.

5. Long-term operating pressures for cylindrical hulls with end-closure restraints should be based upon the maximum strain occurring at one-half the diameter from the closure rather than on the uniform strain found at one diameter or more from the closure. The operating pressure based on maximum strain could be as much as 30% less than the pressure based on strain of an infinite-length cylinder.

ACKNOWLEDGMENT

Mr. John E. Crawford, Research Structural Engineer, NCEL, prepared the finite element analysis of the cylindrical hulls.

Appendix A

CONCRETE PROPORTIONS AND PROPERTIES

The concrete material constituents were portland type III high early strength cement, San Gabriel River Wash aggregate, and fresh water, proportioned as follows: aggregate-to-cement ratio was 3.30 by weight and water-to-cement ratio was 0.55 by weight.

The aggregate was supplied to NCEL kiln dried and bagged. The aggregate was proportioned as shown in Table A-1. All material passed the no. 4 size sieve; therefore, the mix was technically a mortar or microconcrete.

Table A-1. Aggregate Proportions

Sieve Size Designation		Percent Retained
Passing	Retained	
no. 4	no. 8	29.6
no. 8	no. 16	20.8
no. 16	no. 30	14.7
no. 30	no. 50	10.3
no. 50	no. 100	7.3
no. 100	pan	17.3

The concrete compressive strength, modulus of elasticity, and Poisson's ratio are presented in Table A-2. The results were obtained from 3 x 6-inch control cylinders tested under uniaxial compression the same day the cylindrical structure was tested. The concrete used in the hollow cylinder sections had an average compressive strength of approximately 8,830 psi and average secant modulus of elasticity of 3.37×10^6 psi.

Table A-2. Concrete Properties

Specimen No.	Cylinder Section						Hemispherical Caps	
	f'_c (psi)	E_s (psi x 10^6)	E_e (psi x 10^6)	E_p (psi x 10^6)	ν	Age (days)	f'_c (psi)	Age (days)
1	7,860	2.72	2.93	1.37	0.180	127	10,000	147
							8,980	144
2	9,800	3.40	3.63	1.91	0.154	130	9,620	129
							9,270	130
3	9,420	3.47	3.51	2.31	0.150	239	9,190	209
4	9,270	3.75	4.18	2.08	0.155	134	9,870	138
5	5,940	2.40	2.44	1.17	0.125	139	8,620	135
6	5,910	3.07	3.25	1.82	0.150	264	9,600	251
7	9,100	3.45	3.55	2.39	0.172	252	9,640	253
8	9,260	3.36	3.51	1.98	0.167	140	[illegible]	133
9	10,480	3.51	3.68	2.17	0.170	[illegible]	[illegible]	1,127
10	10,640	3.69	3.79	2.06	0.174	60	9,950	1,132
11	8,700	3.82	3.82	2.86	0.120	202	9,950	1,103
12	9,580	3.80	3.85	2.79	0.190	211	9,560	1,237

Note: f'_c = ultimate uniaxial concrete strength.
E_s = secant modulus to strain at 1/2 f'_c.
E_e = elastic modulus for bilinear stress–strain relationship.
E_p = plastic modulus for bilinear stress–strain relationship.
ν = Poisson's ratio of strain at 1/2 f'_c.
Age = age of concrete at time of testing.

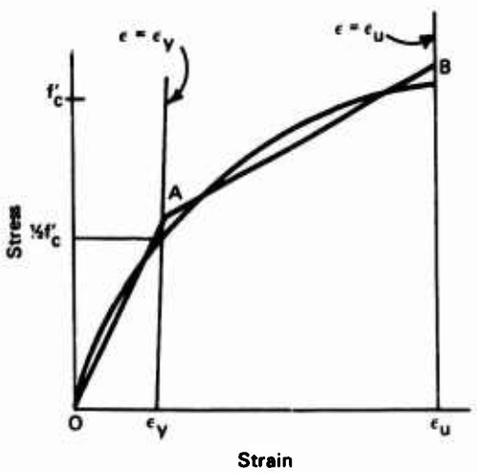

Figure A-1. Construction of bilinear stress–strain curve.

A bilinear stress–strain relation was determined for the concrete of each specimen. An elastic modulus (E_e) and a plastic modulus (E_p) were determined so that the area under the bilinear stress–strain curve was equal to the area beneath the actual curve. As shown in Figure A-1, E_e was found by (1) finding the strain (ϵ_y) at one-half the concrete strength ($1/2\ f'_c$) and drawing a vertical line at ϵ_y ($\epsilon = \epsilon_y$), (2) drawing a straight line (OA) so that the area bounded by OA and line $\epsilon = \epsilon_y$ was equal to the area bounded by the real stress–strain curve and line $\epsilon = \epsilon_y$. The slope of line OA was the E_e. The plastic modulus was found by (1) drawing a vertical line through the ultimate strain ($\epsilon = \epsilon_u$), (2) drawing line AB so that the area bounded by $\epsilon = \epsilon_y$ and line $\epsilon = \epsilon_u$ was equal to the area bounded by the actual stress–strain curve and line $\epsilon = \epsilon_u$. The slope of line AB was E_p.

Appendix B

DRAWINGS OF CYLINDER END CLOSURES

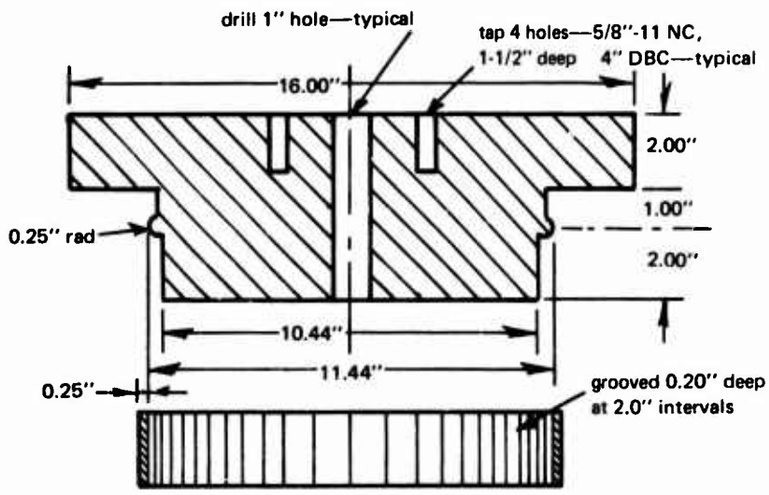

Figure B-1. Pinned end closure and bearing ring.

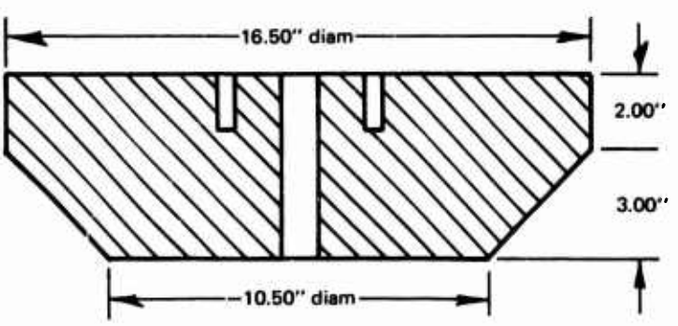

Figure B-2. Beveled end closure.

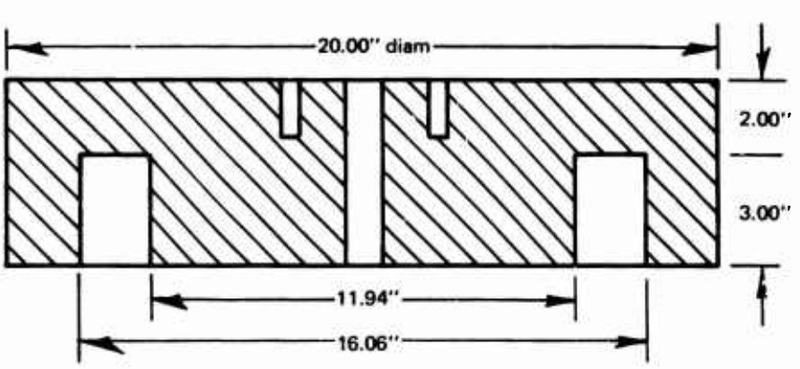

Figure B-3. Fixed end closure.

Appendix C

DISCUSSION OF STRAIN BEHAVIOR ALONG CYLINDER LENGTH

FREE END CLOSURE (SPECIMENS 1 AND 2)

Figures 17 and 18 show that the 1-inch hemispherical end closure affected the behavior of the cylinder. Though the hemisphere provided free end restraint, it induced edge bearing stresses in the cylinder, causing increased strain at a distance of 4 inches from the cylinder edge. Figure 17 shows that at the lower loads the corresponding strains on lines A and B of specimen 1 were the same but at higher loads line B had much higher strains. It is likely that such strain increases were due to nonsymmetry of the cylinder.

Figure 18 shows that the opposite sides of specimen 2 had similar behavior. It appears that the influence of the closure was within a distance of one-half the diameter from the end and that the strains at greater distances were nearly uniform.

The behavior of specimens 1 and 2 indicated that the hemisphere restrained the radial movement of the cylinder at the edge while producing an increased deflection between 2 and 4 inches from the closure. The bearing of the hemisphere on the outer edge of the cylinder produced a shear and moment which increased the radial deflection.

In future design of hemispherical ends, a lower shear distortion and moment would result from centering the bearing surface of the hemisphere on the cylinder wall.

PINNED END CLOSURE (SPECIMENS 3 AND 4)

Figures 19 and 20 show that the pinned end closures provided significant restraint to radial deflection at the cylinder edge. If the cylinders had been fully restrained at the interior, the exterior hoop strains would have been approximately 200 μin./in. at $P/f'_c = 0.20$ because of the radial compressibility of the concrete and the deflection of the steel plate. The actual strains at $P/f'_c = 0.20$ were between 500 and 900 μin./in. These higher strains indicated that the pinned end closure of the model cannot be considered an ideal pinned end but rather one that approximates the pin-type restraint.

At low loads the effect of the closure was limited to a short distance from the end. As the pressure was increased the effect became more pronounced at greater distances. The distance from the edge at which the maximum strain occurred increased as the pressure loading increased. The maximum strains of lines A and B were between 5 and 10 inches from the edge.

The strain gradient between the closure end and the point of maximum strain was nearly the same for both specimens. The gradient indicates a high-shear area between the end and the point of maximum deflection.

BEVELED END CLOSURE (SPECIMENS 5 AND 6)

Figures 21 and 22 show that the beveled end closure provided nearly complete restraint to the radial deflection of the cylindrical hulls. At $P/f'_c = 0.20$, the exterior strains on specimens 5 and 6 at the closure were between 150 and 250 μin./in. Since a 200-μin./in. exterior strain implies zero interior strain, the beveled end closure permitted almost no radial deflection at the cylinder edge. This restraint shows that the closure fit snugly onto the ends, that the cylinders were symmetric at the beveled end, that the epoxy bond between the closure and the cylinder was good, and that little relative movement between the closure and cylinder occurred during test.

The closure affected the cylinder behavior within 16 inches from the edge. The highest strain value was recorded at a distance of one-half the diameter from the edge.

FIXED END CLOSURE (SPECIMENS 7 AND 8)

Figure 23 shows that specimen 7 was significantly restrained at the closure edge. On both lines A and B the strain gradient at the edge indicated a near-zero strain at the joint between the closure and the cylinder. The strain gradient near the edge was steep, with line B showing higher strain values than those of line A. As illustrated in Figure 31, line B had strains considerably greater than the average strain around the circumference of the cylinder.

Figure 24 shows that the response of specimen 8 was similar to that of specimen 7, except that lines A and B had different behavior. The strains on line B tend toward zero strain at the cylinder edge, while the strains on line A do not. This means that at line A the cylinder was not fixed to the end closure at the joint, but the cylinder may be considered fixed at some point within the closure.

On both cylinders the maximum strain occurred between 5 and 10 inches from the cylinder edge and its magnitude was over 4,000 μin./in. Between 2 and 5 inches from the edge there was a strain decrease or a strain plateau. Such behavior was observed only with the fixed end closures and was apparently a result of a moment acting at the closure edge.

Appendix D

DISCUSSION OF CIRCUMFERENTIAL STRAIN

The very large strain difference on specimens 7 and 8 at a distance of 2 inches from the edge indicated that the specimens were out-of-round near the cylinder end and that the fixed end closure did not prevent the unsymmetric deflection of the cylinder near the closure. The fixed closure apparently restrained radial movement at some points and provided no restraint at others. For specimen 7, Figure 31 shows that at 0^{o} (line A) more restraint was provided than at 180^{o} (line B). This behavior corresponded to the difference in the strain along lines A and B given in Figure 23. Similarly the opposite behavior is shown in Figure 32 for specimen 8. On one side of each cylinder the closure acted to provide a fixity, while on the opposite side little restraint was provided. Therefore, the fixed end closure did not provide the total fixity desired.

On specimen 6 the strain difference at 2 inches from the edge was larger than at farther distances. The difference apparently was due to a localized strain increase rather than a general nonsymmetry. Such a sudden development of a high peak strain would not have resulted from a general out-of-round condition; this peak might have been caused by the development of a crack at that point.

Table D-1 summarizes the circumferential strain data by listing the strain difference and mean strain at locations 2, 8, and 16 inches from the edge of the closure and at pressure levels $P/f'_c = 0.10$ and 0.20. In general, the data of Table D-1 show the following:

1. The mean strains indicate that the metal plate end closures restrained the radial deflection near the closure.
2. The similarity in mean strains at 16 inches implies that the effect of the end closures was negligible at a distance of one diameter. from the cylinder edge.
3. Strain differences, therefore out-of-round differences, increased with increasing load.

Table D-1. Maximum Minus Minimum Circumferential Strain and Mean Circumferential Strain at $P/f'_c = 0.10$ and 0.20

Specimen No.	Maximum–Minimum Strain (μin./in.)			Mean Strain (μin./in.)		
	2 Inches From Closure	8 Inches From Closure	16 Inches From Closure	2 Inches From Closure	8 Inches From Closure	16 Inches From Closure
At $P/f'_c = 0.10$						
1	110	190	230	840	790	740
2	230	180	500	1,040	990	1,010
3	280	790	230	700	970	970
4	260	210	90	680	1,000	900
5	430	350	230	360	990	1,000
6	530	400	110	300	630	670
7	340	810	240	110	860	910
8	420	330	390	660	990	840
At $P/f'_c = 0.20$						
1	590	610	860	2,180	2,080	1,940
2	440	700	1,630	2,880	2,800	2,710
3	300	1,060	980	2,760	3,050	2,930
4	800	690	580	1,630	2,870	2,560
5	100[a]	810[a]	520[a]	650[a]	1,800[a]	1,760[a]
6	1,830	1,530	1,070	1,040	1,900	2,340
7	1,240	960	410	1,990	2,710	2,410
8	1,340	1,110	1,070	1,840	3,040	2,540

[a] Strain at $P/f'_c = 0.15$.

REFERENCES

1. Naval Civil Engineering Laboratory. Technical Report R-696: Influence of length-to-diameter ratio on behavior of concrete cylindrical hulls under hydrostatic loading, by H. H. Haynes and R. J. Ross. Port Hueneme, Calif., Sept. 1970. (AD 713088)

2. E. L. Wilson. "Structural analysis of axisymmetric solids," American Institute of Aeronautics and Astronautics, Journal, vol. 3, no. 12, Dec. 1965, pp. 2269-2274.

3. Naval Civil Engineering Laboratory. Technical Report R-588: Behavior of spherical concrete hulls under hydrostatic loading, pt. III. Relationship between thickness-to-diameter ratio and critical pressures, strains, and water permeation rates, by J. D. Stachiw and K. Mack. Port Hueneme, Calif., June 1968. (AD 835492L)

4.——. Technical Report R-679: Failure of thick-walled concrete spheres subjected to hydrostatic loading, by H. H. Haynes and R. A. Hoofnagle. Port Hueneme, Calif., May 1970. (AD 708011)

LIST OF SYMBOLS

D_o	Outside diameter of cylinder (in.)
E_e	Elastic modulus for bilinear stress–strain relationship (psi)
E_p	Plastic modulus for bilinear stress–strain relationship (psi)
E_s	Secant modulus (psi)
f'_c	Ultimate uniaxial compressive concrete strength (psi)
L	Length of cylinder (in.)
L/D_o	Ratio of cylinder length to outside diameter
P	Applied pressure (psi)
P/f'_c	Ratio of applied pressure to concrete strength
P_{im}	Implosion pressure (psi)
P_{im}/f'_c	Ratio of implosion pressure to concrete strength
r_i	Interior radius of cylinder (in.)
r_o	Exterior radius of cylinder (in.)
t	Thickness of cylinder wall (in.)
t/D_o	Ratio of cylinder wall thickness to outside diameter
ϵ	Strain (in./in.)
ϵ_u	Ultimate strain (in./in.)
ϵ_y	Yield strain (in./in.)
ν	Poisson's ratio

Naval Civil Engineering Laboratory
INFLUENCE OF END-CLOSURE STIFFNESS ON BEHAVIOR OF CONCRETE CYLINDRICAL HULLS SUBJECTED TO HYDROSTATIC LOADING, by L. F. Kahn
TR-740 53 p. illus October 1971 Unclassified

1. Concrete hulls I. 3.1610-1

Twelve model concrete cylindrical hulls were subjected to hydrostatic loading to determine the influence of end-closure stiffness on implosion pressure and strain behavior of the cylinders. Results showed that variation of end-closure stiffness did not reduce the implosion pressure below that of a cylinder with a free end condition or below the implosion pressure predicted by elastic thick-wall theory. To vary the closure stiffness, concrete hemisphere and steel plate end closures were used to simulate free, pinned, beveled, and fixed end conditions. Strain variations along the length of the cylinders indicated that the influence of the closure was limited to a distance of one diameter from the closure. Recommendations are presented to aid in the design of concrete cylindrical hulls.

Naval Civil Engineering Laboratory
INFLUENCE OF END-CLOSURE STIFFNESS ON BEHAVIOR OF CONCRETE CYLINDRICAL HULLS SUBJECTED TO HYDROSTATIC LOADING, by L. F. Kahn
TR-740 53 p. illus October 1971 Unclassified

1. Concrete hulls I. 3.1610-1

Twelve model concrete cylindrical hulls were subjected to hydrostatic loading to determine the influence of end-closure stiffness on implosion pressure and strain behavior of the cylinders. Results showed that variation of end-closure stiffness did not reduce the implosion pressure below that of a cylinder with a free end condition or below the implosion pressure predicted by elastic thick-wall theory. To vary the closure stiffness, concrete hemisphere and steel plate end closures were used to simulate free, pinned, beveled, and fixed end conditions. Strain variations along the length of the cylinders indicated that the influence of the closure was limited to a distance of one diameter from the closure. Recommendations are presented to aid in the design of concrete cylindrical hulls.

Naval Civil Engineering Laboratory
INFLUENCE OF END-CLOSURE STIFFNESS ON BEHAVIOR OF CONCRETE CYLINDRICAL HULLS SUBJECTED TO HYDROSTATIC LOADING, by L. F. Kahn
TR-740 53 p. illus October 1971 Unclassified

1. Concrete hulls I. 3.1610-1

Twelve model concrete cylindrical hulls were subjected to hydrostatic loading to determine the influence of end-closure stiffness on implosion pressure and strain behavior of the cylinders. Results showed that variation of end-closure stiffness did not reduce the implosion pressure below that of a cylinder with a free end condition or below the implosion pressure predicted by elastic thick-wall theory. To vary the closure stiffness, concrete hemisphere and steel plate end closures were used to simulate free, pinned, beveled, and fixed end conditions. Strain variations along the length of the cylinders indicated that the influence of the closure was limited to a distance of one diameter from the closure. Recommendations are presented to aid in the design of concrete cylindrical hulls.

Naval Civil Engineering Laboratory
INFLUENCE OF END-CLOSURE STIFFNESS ON BEHAVIOR OF CONCRETE CYLINDRICAL HULLS SUBJECTED TO HYDROSTATIC LOADING, by L. F. Kahn
TR-740 53 p. illus October 1971 Unclassified

1. Concrete hulls I. 3.1610-1

Twelve model concrete cylindrical hulls were subjected to hydrostatic loading to determine the influence of end-closure stiffness on implosion pressure and strain behavior of the cylinders. Results showed that variation of end-closure stiffness did not reduce the implosion pressure below that of a cylinder with a free end condition or below the implosion pressure predicted by elastic thick-wall theory. To vary the closure stiffness, concrete hemisphere and steel plate end closures were used to simulate free, pinned, beveled, and fixed end conditions. Strain variations along the length of the cylinders indicated that the influence of the closure was limited to a distance of one diameter from the closure. Recommendations are presented to aid in the design of concrete cylindrical hulls.

Naval Civil Engineering Laboratory
INFLUENCE OF END-CLOSURE STIFFNESS ON BEHAVIOR OF CONCRETE CYLINDRICAL HULLS SUBJECTED TO HYDROSTATIC LOADING, by L. F. Kahn
TR-740 53 p. illus October 1971 Unclassified

1. Concrete hulls I. 3.1610-1

Twelve model concrete cylindrical hulls were subjected to hydrostatic loading to determine the influence of end-closure stiffness on implosion pressure and strain behavior of the cylinders. Results showed that variation of end-closure stiffness did not reduce the implosion pressure below that of a cylinder with a free end condition or below the implosion pressure predicted by elastic thick-wall theory. To vary the closure stiffness, concrete hemisphere and steel plate end closures were used to simulate free, pinned, beveled, and fixed end conditions. Strain variations along the length of the cylinders indicated that the influence of the closure was limited to a distance of one diameter from the closure. Recommendations are presented to aid in the design of concrete cylindrical hulls.

Naval Civil Engineering Laboratory
INFLUENCE OF END-CLOSURE STIFFNESS ON BEHAVIOR OF CONCRETE CYLINDRICAL HULLS SUBJECTED TO HYDROSTATIC LOADING, by L. F. Kahn
TR-740 53 p. illus October 1971 Unclassified

1. Concrete hulls I. 3.1610-1

Twelve model concrete cylindrical hulls were subjected to hydrostatic loading to determine the influence of end-closure stiffness on implosion pressure and strain behavior of the cylinders. Results showed that variation of end-closure stiffness did not reduce the implosion pressure below that of a cylinder with a free end condition or below the implosion pressure predicted by elastic thick-wall theory. To vary the closure stiffness, concrete hemisphere and steel plate end closures were used to simulate free, pinned, beveled, and fixed end conditions. Strain variations along the length of the cylinders indicated that the influence of the closure was limited to a distance of one diameter from the closure. Recommendations are presented to aid in the design of concrete cylindrical hulls.

Naval Civil Engineering Laboratory
INFLUENCE OF END-CLOSURE STIFFNESS ON BEHAVIOR OF CONCRETE CYLINDRICAL HULLS SUBJECTED TO HYDROSTATIC LOADING, by L. F. Kahn
TR-740 53 p. illus October 1971 Unclassified

1. Concrete hulls I. 3.1610-1

Twelve model concrete cylindrical hulls were subjected to hydrostatic loading to determine the influence of end-closure stiffness on implosion pressure and strain behavior of the cylinders. Results showed that variation of end-closure stiffness did not reduce the implosion pressure below that of a cylinder with a free end condition or below the implosion pressure predicted by elastic thick-wall theory. To vary the closure stiffness, concrete hemisphere and steel plate end closures were used to simulate free, pinned, beveled, and fixed end conditions. Strain variations along the length of the cylinders indicated that the influence of the closure was limited to a distance of one diameter from the closure. Recommendations are presented to aid in the design of concrete cylindrical hulls.

Naval Civil Engineering Laboratory
INFLUENCE OF END-CLOSURE STIFFNESS ON BEHAVIOR OF CONCRETE CYLINDRICAL HULLS SUBJECTED TO HYDROSTATIC LOADING, by L. F. Kahn
TR-740 53 p. illus October 1971 Unclassified

1. Concrete hulls I. 3.1610-1

Twelve model concrete cylindrical hulls were subjected to hydrostatic loading to determine the influence of end-closure stiffness on implosion pressure and strain behavior of the cylinders. Results showed that variation of end-closure stiffness did not reduce the implosion pressure below that of a cylinder with a free end condition or below the implosion pressure predicted by elastic thick-wall theory. To vary the closure stiffness, concrete hemisphere and steel plate end closures were used to simulate free, pinned, beveled, and fixed end conditions. Strain variations along the length of the cylinders indicated that the influence of the closure was limited to a distance of one diameter from the closure. Recommendations are presented to aid in the design of concrete cylindrical hulls.